Journal Of Anatomy
February 2023, Volume 242 Issue 2 Pages 312-326
https://doi.org/10.1111/joa.13763
https://archimer.ifremer.fr/doc/00927/103851/

The anatomy of the head muscles in caecilians (Amphibia: Gymnophiona): Variation in relation to phylogeny and ecology?

Lowie Aurélien [1], De Kegel Barbara [1], Wilkinson Mark [2], Measey John [3], O'Reilly James C. [4], Kley Nathan J. [5], Gaucher Philippe [6], Adriaens Dominique [1], Herrel Anthony [1, 7]

[1] Ghent University, Department of Biology, Evolutionary Morphology of Vertebrates, Ghent, Belgium
[2] Department of Life Sciences, Natural History Museum, London, UK
[3] Centre for Invasion Biology, Department of Botany & Zoology, Stellenbosch University, Stellenbosch, South Africa
[4] Department of Biomedical Sciences, Ohio University, Cleveland Campus, Cleveland, Ohio, USA
[5] Department of Anatomical Sciences, Health Sciences Center, Stony Brook University, Stony Brook, New York, USA
[6] USR 3456, CNRS, Centre de recherche de Montabo IRD, Cayenne, France
[7] UMR 7179 C.N.R.S/M.N.H.N., Département d'Ecologie et de Gestion de la Biodiversité, Paris Cedex 5, France

* Corresponding author : Aurélien Lowie, email address : aurelien.lowie@ugent.be

Abstract :

In limbless fossorial vertebrates such as caecilians (Gymnophiona), head-first burrowing imposes severe constraints on the morphology and overall size of the head. As such, caecilians developed a unique jaw-closing system involving the large and well-developed m. interhyoideus posterior, which is positioned in such a way that it does not significantly increase head diameter. Caecilians also possess unique muscles among amphibians. Understanding the diversity in the architecture and size of the cranial muscles may provide insights into how a typical amphibian system was adapted for a head-first burrowing lifestyle. In this study, we use dissection and non-destructive contrast-enhanced micro-computed tomography (mu CT) scanning to describe and compare the cranial musculature of 13 species of caecilians. Our results show that the general organization of the head musculature is rather constant across extant caecilians. However, the early-diverging Rhinatrema bivittatum mainly relies on the 'ancestral' amphibian jaw-closing mechanism dominated by the m. adductores mandibulae, whereas other caecilians switched to the use of the derived dual jaw-closing mechanism involving the additional recruitment of the m. interhyoideus posterior. Additionally, the aquatic Typhlonectes show a greater investment in hyoid musculature than terrestrial caecilians, which is likely related to greater demands for ventilating their large lungs, and perhaps also an increased use of suction feeding. In addition to three-dimensional interactive models, our study provides the required quantitative data to permit the generation of accurate biomechanical models allowing the testing of further functional hypotheses.

Keywords : 3D model, burrowing, cranial morphology, limbless, muscle architecture, myology

Introduction

The cranial system of tetrapods plays vital roles in many activities such as feeding and lung ventilation, in addition to housing and protecting the brain and major sensory organs (Wake, 1993). In limbless fossorial vertebrates such as caecilians (Gymnophiona), head-first burrowing imposes additional constraints on the cranial system (O'Reilly, 2000; Wake, 1993). Indeed, their typically compact and robust crania, with some bones joined together via tight sutures and others fully fused together, have been interpreted as adaptations for head-first burrowing (e.g. Wake, 1993; Wake and Hanken, 1982; Wilkinson, 2012). However, unexpectedly, investigations of the impact of burrowing forces on skull shape have found no direct relationship between the external forces experienced during burrowing and skull shape (Ducey *et al.*, 1993; Herrel and Measey, 2010; Kleinteich *et al.*, 2012; Lowie *et al.*, 2021). Rather, cranial shape variation appears more constrained by the jaw adductor muscles in relation to feeding (Lowie *et al.*, 2022).

A burrowing lifestyle imposes severe constraints on the external diameter of the head in head-first burrowing vertebrates (e.g. Bemis *et al*., 1983; Gans, 1974; O'Reilly, 2000), and thus upon their cephalic musculature. For instance, in caecilians, the lateral external adductors are constrained in size by adjacent bones and thus are strongly reduced compared to those of other amphibians (Bemis *et al*., 1983; Nussbaum, 1977; Nussbaum, 1983; O'Reilly, 2000). However, among limbless burrowing tetrapods, caecilians evolved a unique jaw-closing system involving the large and well-developed *m. interhyoideus posterior* (MIHP), positioned in such a way that it does not significantly increase head diameter (Herrel *et al*., 2019; Nussbaum, 1977; Nussbaum, 1983; O'Reilly, 2000). Additionally, apart from their unique and transformed MIHP, caecilians also possess muscles that are not present in other amphibians (i.e. a true *m. pterygoideus* and the *m. levator quadrati*; e.g. Kleinteich and Haas, 2007, Nussbaum, 1977; Wilkinson and Nussbaum 1997).

Although their cranial osteology has been well documented (e.g. Bardua *et al.*, 2019; Lowie *et al.*, 2021; Sherratt *et al.*, 2014; Taylor; 1969; Wake, 1993; Wiedersheim, 1879; Wilkinson and Nussbaum, 1997), studies on the diversity of cranial musculature of caecilians are more scarce. Several studies described the cranial and hyobranchial musculature in various developmental stages, including larvae (e.g. Haas, 2001; Kleinteich and Haas, 2011, 2007; Müller *et al*., 2009; Theska *et al*., 2018), but descriptions of the cranial musculature in adults are limited (but see Bemis *et al*., 1983; Carroll, 2007; Lowie *et al*., 2022; Nussbaum, 1983, 1977; O'Reilly, 2000; Wilkinson and Nussbaum, 1997). Yet, understanding the diversity in the architecture and size of the cranial muscles may provide insights into how a typical amphibian system was adapted for a head-first burrowing lifestyle. Moreover, given that some caecilians are more surface dwelling (e.g. Kupfer *et al.*, 2005; Ramaswami, 1941), whereas others are

active burrowers (e. g. Dunn, 1942; Maciel *et al.*, 2012) or even fully aquatic (e. g. Dunn, 1942; Verdade *et al.*, 2000), one can expect variation in the investment in the different groups of head muscles.

In this study, we describe and compare the cranial musculature in 13 species of caecilians using both dissections and non-destructive contrast-enhanced micro-computed tomography (µCT) scanning. Our study further provides a three-dimensional atlas of the head musculature of caecilians, while also pointing out variation related to phylogeny and ecology. As suggested by Herrel *et al*. (2019), quantitative data are essential to link variation in form with variation in function. As proportions of the different muscles tend to vary across caecilians (Lowie *et al*., 2022; O'Reilly, 2000), in addition to the qualitative description of the musculature, we further provide and compare the volume and physiological cross-sectional area (PCSA) of head muscles across caecilians. We predict that terrestrial species will show larger jaw adductors whereas aquatic species will show better developed hyoid muscles used for buccal pumping and during compensatory suction feeding (Carrier and Wake, 1995; O'Reilly, 2000; Wilkinson and Nussbaum, 1997). Additionally, following Nussbaum (1977; 1983), we hypothesize that the earliest-diverging lineages, such as rhinatrematids, can be expected to show a more generalized amphibian morphology with relatively large adductors and a small *m. interhyoideus posterior* and we test these predictions quantitatively.

Material and methods

Specimens

We describe and quantify the head musculature of 44 individuals from 13 species of caecilians belonging to seven out of the 10 currently recognized families (Table 1, Fig. S1), thus capturing a broad diversity in cranial osteology, phylogeny and ecology. Our sample was restricted to adults and included both males and females. Although sexual dimorphism has been documented in some caecilians (e.g. Kupfer, 2009; Nussbaum and Pfrender, 1998), interspecific variation largely exceeds the sex-specific variation (Sherratt *et al*., 2014). Specimens were primarily obtained from our personal collections and completed with specimens from museum collections (Table S1).

Dissection and muscle properties

We examined five head muscles that contribute to the unique dual jaw-closing system in caecilians (Nussbaum, 1983; Fig. 1A,B): the *m. adductor mandibulae internus* (MAMI)*, longus* (MAML)*,* and *articularis* (MAMA)*,* the *m. interhyoideus posterior* (MIHP), and the *m. pterygoideus* (MPt)*.* Additionally, the well-developed jaw opener, the *m. depressor mandibulae* (MDM), the *m. levator quadrati* (MLQ), the *m. interhyoideus anterior* (MIHA), and the *m. intermandibularis* (MIM) were included (Fig. 1A). Although the muscles of the hyobranchial apparatus innervated by the

glossopharyngeal (IX) and vagus (X) nerves were not examined here (but see Kleinteich and Haas, 2007), three muscles innervated by the hypoglossal nerve —i.e. the *m. genioglossus* (MGG), *m. geniohyoideus* (MGH), and *m. rectus cervicis* (MRC)—were included in our study (Fig. 1B). The muscle nomenclature used here follows Kleinteich and Haas (2007), which is based on the putative homologies with jaw musculature in other amphibians and in caecilian larvae (Haas, 2001; Kleinteich and Haas, 2007).

Prior to dissection, specimens used for morphological analyses that were stored in a 70% aqueous ethanol solution were rehydrated in water for 15–20 min. Muscles were removed unilaterally on each specimen under a dissecting microscope (Wild M3Z, Wild Inc., Switzerland) and weighed using a digital microbalance (Sartorius CP225D ± 10 µg). Muscle fibre lengths were obtained by submerging the muscles in a 30% nitric acid solution (HNO_3 30%) for 24 h to dissolve all connective tissue. Muscle fibres were then put in a 50% glycerol solution and at least 10 fibres for every muscle were drawn using a dissecting microscope equipped with a *camera lucida.* Drawings were then scanned and fibre lengths were quantified using ImageJ 1.52a (Wayne Rasband, National Institutes of Health, USA). Next, we calculated the average length of the fibres for each muscle. Finally, the physiological cross-sectional area (PCSA) of each muscle was calculated as follows:

$$PCSA = \frac{musclemass * cos(pennationangle)}{musculardensity * fibrelength}$$

where muscle mass is in g, pennation angle is in rad, muscular density is in g cm^{-3} and fibre length is in cm. A muscular density of 1.06 g cm^{-3} (Mendez and Keys, 1960) was used. Pennation angles were obtained from the contrast-enhanced micro-computed tomography (µCT) scans (see 'µCT imaging' below). A full summary of the muscle measurements is provided in Table S2.

µCT imaging

Micro-CT scans of 12 different species were used for this study (*T. compressicauda* could not be scanned and the closely related *T. natans* was used instead; Supplementary Table S3). All the scans were performed at the Centre for X-Ray Tomography at Ghent University, Belgium (UGCT, www.ugct.ugent.be) using the HECTOR micro-computed tomography (µCT) scanner (Masschaele *et al*., 2013). The scanner settings were sample dependent. The tube voltage varied between 100 and 120 kV and the number of X-ray projections taken over 360° was typically about 2000 per scan. The isotropic voxel sizes for all scans are listed in Table S3. All the µCT scans were processed using both automatic thresholding and manual segmentation to reconstruct the cranium and mandible in 3D using Amira 2019.3 (Visage Imaging, San Diego, CA, USA). Using Geomagic Wrap (3D systems), surfaces were

prepared by removing highly creased edges and spikes, and decimated to a maximum of approximately 700,000 faces to reduce computational demands without compromising details.

Next, these specimens were prepared for soft-tissue visualization (Table S3). Specimens were stained using either a 2.5% phosphomolybdic acid (PMA; Descamps *et al.*, 2014) solution or a 6% Lugol's iodine (I_2KI; Gignac *et al.*, 2016) solution when a permanent blue coloration was not allowed. The staining time varied from 14 to 21 days depending on the size of the specimen. All these specimens were then scanned again with the HECTOR µCT scanner (100 kV, 2400 projections; Table S2). After a fully manual segmentation in Amira 2019.3, muscles volumes were computed using the 'Material Statistics' module. The contrast threshold was then manually lowered for each muscle in order to highlight muscles fibres. Fibre lengths of all the muscles and pennation angles of the *m. interhyoideus posterior* and the *m. depressor mandibulae* were measured using the standard measure tool in Amira. Average fibre lengths and pennation angles were calculated based on at least 10 fibres per muscle. The physiological cross-sectional area (PCSA) was then calculated by dividing muscle volume by muscle length and multiplied by the cosine of the pennation angle where relevant (Table S2).

Muscle volume and PCSA (proportional to muscle force output) were then compared across caecilian phylogeny (Jetz and Pyron, 2018). Total muscular volume and PCSA were computed for each species and the relative proportion of each muscle was then calculated. For simplicity, muscles were grouped in different functional groups and compared across species. The first functional group includes all the muscles that play a function in jaw motion (MAMA, MAML, MAMI, MIHP, MDM, MPt and MLQ), whereas the second group includes muscles that play a role in hyoid movements (MGG, MGH, MRC, MIM and MIH). Then, to compare the contribution of the traditional vs. derived jaw closers, the adductors were included in one group (MAMA, MAML and MAMI) and compared to the MIHP. Finally, to get a global overview of the muscular distribution across caecilians, the 12 muscles were split in five groups: traditional jaw adductors (MAMA, MAML and MAMI), the derived jaw adductor (MIHP), jaw stabilisers (MLQ and MPt), jaw opener (MDM), and hyoid muscles (MGG, MGH, MRC, MIM and MIH).

Visualization

All the illustrations used in this publication were prepared using Blender v3.1.0 (Blender Foundation, Amsterdam). For each specimen, unstained and stained surfaces were merged and aligned using visible landmarks in both datasets to create a single musculoskeletal model for each specimen. Next, filters were applied to enhance the visualization and the discrimination of both hard and soft tissues. Artificial muscles fibres were also included in order to help visualise pennation where present (pennate muscle material modified from procedural feather material by Sai Charan). Additionally, a 3D model of *Caecilia*

tentaculata was uploaded on Sketchfab (https://sketchfab.com), and a custom viewer was used to allow showing and hiding parts of the model (https://github.com/Croisened/SketchFabShowAndHide).

Results

Muscular anatomy

The general description of the musculature is based on a specimen of *Caecilia tentaculata* and applies to the 13 species examined, with exceptions and variations on the general design noted where present. The interactive 3D models of the early-diverging *Rhinatrema bivittatum* and the *Caecilia tentaculata* used as reference can be accessed through github (https://github.com/Aurelien-UGent/3D_Models/).

Hyoid muscles innervated by the facial nerve (VII)

In larvae, the hyoid musculature consists of the *m. depressor mandibulae*, the *m. levator hyoidei*, the *m. hyomandibularis,* and the *mm. interhyoidei anterior* and *posterior* (Kleinteich and Haas, 2007). However, in adults, the *m. hyomandibularis* and *m. levator hyoidei* are probably partly incorporated into the *m. depressor mandibulae* and the *m. pterygoideus*, respectively (Kleinteich and Haas, 2007), and as such, no trace of the *m. hyomandibularis* or *m. levator hyoidei* were observed in the adult specimens studied here.

M. depressor mandibulae (MDM)

This large muscle lies lateral to the squamosal and, as such, partly covers it. Posteriorly, it also covers the ascending process of the quadrate and the anterior trunk musculature. Anteriorly, it originates from a ridge on the lateral side of the squamosal; dorsally it originates from the posterodorsal surface of the parietal with some fibres originating from a fascia overlying the anterior dorsal trunk musculature. It inserts on the dorsal and medial sides of the retroarticular process (RAP), and is thus an antagonist of the adductor muscles as its function is to open the jaws. Although this muscle is often subdivided into two distinct parts in larvae (Kleinteich and Haas, 2007), the posterior and anterior parts appear largely fused in adult caecilians. However, in C. *tentaculata*, *R. bivittatum* and *G. seraphini*, although fused, the two parts could be clearly identified thanks to the orientation of the fibres (Fig. 2A). The most posterior and medial part of the *m. depressor mandibulae* (*pars profundus;* Wilkinson and Nussbaum, 1997) consists of vertically oriented fibres and has a medial, and more rostral, insertion on the retroarticular process. The anterior and more lateral part (*pars superficialis;* Wilkinson and Nussbaum, 1997) consists of more horizontally oriented fibres inserting on the dorsal side of the retroarticular process. In the other species included in this study the MDM mostly consists of a single muscle (Fig. 2B).

In the phylogenetically basal *R. bivittatum* (Fig. S1), this muscle is large compared to the small retroarticular process on which it inserts. Similar to other caecilians, the most anterior part of the MDM originates from the lateral ridge of the squamosal. However, the posterior part does not originate on the parietal bone, which is entirely covered by the adductor muscles, but instead inserts on its antimere at the midline of the dorsal trunk musculature via a raphe. Its insertion on the retroarticular process is similar to that of other caecilians. The MDM of *R. bivittatum* and also *I. kohtaoensis* wraps around the retroarticular process and not only inserts on the medial and dorsal surfaces thereof, but also on its lateral surface (Fig. 2C).

In the aquatic *T. natans*, the MDM consists of a long and thin sheet of almost horizontal muscle fibres. They mainly originate from the anterolateral part of the squamosal, like in other caecilians, but their dorsal origin is limited to a small anterolateral part of the parietal bone. Additionally, the MDM only inserts on the dorsal side of the retroarticular process (Fig. 2D).

M. interhyoideus posterior **(MIHP)**

Along with the jaw adductors, this muscle is part of the unique dual jaw-closing mechanism found in caecilians (Nussbaum, 1977; Nussbaum, 1983). Lying posteroventrally to the *m. depressor mandibulae*, this muscle is the most lateral muscle in the neck region. Caudally and ventrally, it originates from a fascia attached to, respectively, the lateral and ventral musculature of the body. As reported by Wilkinson and Nussbaum (1997) in typhlonectids and Nussbaum (1977) in rhinatrematids and ichthyophiids, some deep fibres are also inserting on the *m. obliquus externus* via a septum. This large muscle inserts on the most caudal part of the ventral side of the retroarticular process, close to its tip. This fan-shaped muscle inserts on the retroarticular process directly via muscle fibres but also via a central tendon on which obliquely oriented fibres insert (Fig. 3A). Except in *I. kohtaoensis* and *R. bivittatum*, this elongate muscle runs along the long axis of the body.

In *I. kohtaoensis*, the morphology of the MIHP is quite different from that in the other species. This muscle is smaller and more ventrally projecting. Additionally, the central tendon, and the pennation angle of the muscle fibres, are smaller than in other species (e.g. *C. tentaculata*), resulting in an almost superficially positioned, parallel-fibred, tendonless muscle (Fig. 3B).

Unlike all of the other caecilians included in our study, no central tendon was found in the MIHP of *R. bivittatum*. As previously observed (Nussbaum, 1977; Nussbaum, 1983), all the fibres insert directly on the retroarticular process. Moreover, similarly to the condition exhibited by *I. kohtaoensis*, the muscle is oriented strongly ventrally (Fig. 3C).

M. interhyoideus anterior **(MIHA)**

The *m. interhyoideus anterior* lies anterior to the *m. interhyoideus posterior*, and posterior to the *m. intermandibularis*. The most anterior part of the MIHP often overlaps with the most posterior part of the MIHA, which is positioned more medially. The muscle originates from the ventral side of the body, from a midline raphe and inserts on the ventral side of the retroarticular process, anterior to the insertion of the *m. interhyoideus posterior* (Fig. 3). Although far smaller than the *m. interhyoideus posterior*, this muscle with ventromedially oriented muscle fibres has been suggested to be involved in the closing of the jaws as well as in buccopharyngeal pumping (Carrier and Wake, 1995). Although hardly divisible from the MIHP in the stained µCT scans in some species, its separation from the MIHP was always evident during dissection. Note, however, that some authors have reported that the separation is not always clear in some species (Wilkinson and Nussbaum, 1997).

Jaw muscles innervated by the trigeminal nerve (V)

The mandibular musculature consists of the adductor complex, the *m. intermandibularis* (MIM) and the *m. pterygoideus* (MPt). The adductor complex is responsible for closing the jaws and includes the *m. adductor mandibulae longus* (MAML)*, internus* (MAMI) and *articularis* (MAMA), and the *levator quadrati* (MLQ). In stegokrotaphic caecilians, the whole adductor group is constrained in the adductor chamber by the quadrato-squamosal complex and maxillopalatine bones (Fig. 4A; Bemis *et al*., 1983; Nussbaum, 1983, 1977; O'Reilly, 2000). Each subdivision of the adductors is separated by a ramus of the trigeminal nerve; the mandibular branch separates the MAMA from the MAML and the maxillary branch separates the MAML from the MAMI (Haas, 2001).

***M. adductor mandibulae longus* (MAML)**

This is the largest muscle of the adductor group, located medial to the squamosal. It originates from the ventral surfaces of the lateral edges of the parietal and frontal bones, and as such, is nested under the skull roof. The MAML inserts on the most anterodorsal part of the pseudoangular, at the anterior extreme of the *canalis primordialis*. Muscular fibres are vertically oriented and converge from the broad site of origin toward their narrower insertion on the pseudoangular (Fig. 4B).

In caecilian species with a zygokrotaphic skull condition, i.e. having an opened temporal region such as *G. seraphini, T. natans* and *R. bivittatum*, although the most anterior origin of this muscle is still nested in a groove under the frontal bone, the middle to posterior fibres take their origin from the dorsolateral surface of the parietal bone (Fig. 5).

In *R. bivittatum*, three muscular bundles were identified between the mandibular and maxillary branches of the trigeminal nerve, and as such, belong to the MAML. The central one is by far the largest and possesses a large oblique tendon, on which fibres originating from the dorsal midline of the frontal

and parietal bones are inserted (Fig. 6A). This tendon in the MAML is unique among the caecilians examined. It inserts on the most posterodorsal part of the pseudodentary. Additionally, two separate small bundles of vertical fibres, on each side of the central bundle, insert on the medial edge of the *canalis primordialis*. The origin of the lateral bundle is on the medial surface of the squamosal bone, whereas the origin of the medial bundle is on the lateral surface of the *os basale* (Fig. 6A–B).

***M. adductor mandibulae internus* (MAMI)**

This muscle is located medial to the *m. adductor mandibulae longus*. It originates on the most anterior part of the dorsolateral region of the *os basale*, ventral to the origin of the *m. adductor mandibulae longus*. Anteriorly, a few fibres also originate from the lateral surface of the sphenethmoid (Fig. 3C, *C. tentaculata*). It inserts, through a long and thin bundle of vertical muscle fibres terminating in a tendon, on the medial side of the retroarticular process.

In *I. kohtaoensis* and *T. natans*, this muscle takes its origin more anteriorly and more fibres take their origin on the lateral side of the sphenethmoid bone (Fig. 7). In *B. taitanus*, a true MAMI could not be identified and is probably fused with the MAML.

In *R. bivittatum*, two muscle bundles of obliquely oriented fibres could be identified. The biggest part originates anteriorly from the lateral surface of the sphenethmoid bone, whereas the posterior part takes its origin on the lateral surface of the *os basale*. Both are inserted on a thin tendon inserting on the medial part of the pseudoangular, just posterior to the foramen of the *ramulus intermandibularis* (Fig. 6C).

***M. adductor mandibulae articularis* (MAMA)**

This muscle is the most posterior of the three adductors and consists of vertically oriented fibres. Located medial to the quadrate bone, it originates from the medial surface of the quadrate and inserts on the dorsal surface of the pseudo-angular, on the posterolateral ridge of the *canalis primordialis*, just anterior to the jaw articulation (Fig. 4E).

In *R. bivittatum*, although the insertion of the MAMA is similar to that of the other caecilians examined, its origin is more anterior, resulting in a relatively long MAMA with obliquely oriented fibres. Indeed, the MAMA originates from the medial surface of the anterior part of the squamosal bone (Fig. 6D).

***M. levator quadrati* (MLQ)**

This muscle is positioned medial to the m. *adductor mandibulae internus.* It originates from the lateral region of the *os basale*, ventral and posterior to the area of origin of the MAMI, and inserts on the dorsolateral side of the pterygoid process of the quadrate. This is a small and parallel-fibred muscle

(Fig. 4D). Its function is to contribute to streptostylic rotation of the quadrate, and also likely stabilize it as well (Kleinteich *et al*., 2008). In *T. natans* and *R. bivittatum,* no *m. levator quadrati* could be identified.

***M. pterygoideus* (MPt)**

This muscle consists of fibres running along the ventromedial surface of the lower jaw and wrapping around the *processus internus* of the mandible. These fibres originate, through an aponeurosis, from the ventral side of the pterygoid process of the quadrate and inserts medially along the ventral side of the retroarticular process (Fig. 8A). Its suggested function is to move the pterygoid process of the quadrate in a ventrocaudal direction and the muscle likely participates in jaw closing at large gape angles. Note that unlike teresomatan caecilians, rhinatrematids and ichthyophiids have large pterygoids with small pterygoid processes of the quadrate, which likely impacts upon the origin of this muscle (MW pers. obs.)

In *R. bivittatum*, the MPt is relatively bulky, and not only inserts on the ventral side of the retroarticular process, but also on the lateral and medial sides of it. Unlike in other caecilians, the pterygoid of *R. bivittatum* possesses a distinct ventral process from which the MPt fibres directly originate (Fig. 8B). Additionally, a separate bundle of fibres originating from the lateral surface of the pterygoid bone inserts into a depression on the anteromedial side of the *processus internus* of the mandible (Fig. 8C). Similarly, *I. kohtaoensis* also possess an additional pterygoid muscle consisting of a really thin sheet of vertical fibres originating from the pterygoid process of the quadrate and inserting on the medial surface of the pseudoangular, anterior to the *processus internus* of the mandible.

In *T. natans*, the MPt is so big that it wraps dorsally around the stapes and the *os basale* to insert on the ventrolateral surface of the pterygoid process of the quadrate. As observed *in R. bivittatum* and *I. kohtaoensis*, some short fibres also insert into a depression on the anteromedial side of the *processus internus* of the mandible. Additionally, as reported in other tyhplonectids (Wilkinson and Nussbaum, 1997), some fibres of the MPt also originates from the ventral surface of the basipterygoid process of the *os basale*.

***M. intermandibularis* (MIM)**

This superficial fan-shaped muscle is the most ventral muscle of the head and consists of ventromedially oriented fibres. It has a broad origin on the medial side of the pseudoangular, anterior to the insertion site of the *m. pterygoideus*, and its anteriormost fibres run along the pseudoangular to insert, via a central raphe of variable length at the lingual surface of the most rostral part of the mandible, just next to the mandibular symphysis. More posterior fibres of the *m. intermandibularis*

insert with those of its antimere at a midline raphe (Fig. 9A). Its function is to move the buccal floor and as such is involved in the buccal pump of caecilians (Carrier and Wake, 1995) and perhaps in feeding as well (Wilkinson and Nussbaum, 1997).

In *G. seraphini*, an additional bundle of fibres can be observed ventral to the MIM. The muscle fibres run anteroposteriorly and originate from the medial surface of the pseudoangular, just ventral to the origin of the MIM. This muscle inserts onto the MIM and is likely a MIM posterior (Fig. 9B).

Muscles innervated by the hypoglossal nerve

This group comprises tongue and hyoid muscles: the *m. genioglossus*, the *m. geniohyoideus*, and *the m. rectus cervicis*. Although variation in these muscles was limited in the specimens examined, some variation has previously been reported (e.g. Wilkinson and Nussbaum, 1997). As such, future studies would benefit from a more detailed investigation into the variation of these muscles.

***M. genioglossus* (MGG)**

This is a loose bundle of diffuse fibres that forms the muscular part of the tongue. It originates from the lingual surface of the pseudodentary, near the mandibular symphysis, and terminates beneath the lingual epithelium (Fig. 10A). This muscle likely plays a role in tongue movements.

***M. geniohyoideus* (MGH)**

This muscle consists of a longitudinal band located between the *m. genioglossus* and the *m. intermandibularis*. It originates from the lingual surface of the pseudodentary, ventral to the *m. genioglossus*, and inserts on the anteroventral surface of ceratobranchial I, and on the *m. rectus cervicis* at the level of ceratobranchial I/II (Fig. 10B). This muscle is involved in buccopharyngeal pumping (Carrier and Wake, 1995) and hyoid/tongue protraction.

***M. rectus cervicis* (MRC)**

The *m. rectus cervicis* lies in line with the *m. geniohyoideus* caudally. It originates from a fascia with the *m. geniohyoideus* but also from the posteroventral surface of ceratobranchial I and inserts on the *m. rectus abdominis* at the level of ceratobranchial III/IV (Fig. 10B). This muscle is involved in buccal expansion (Carrier and Wake, 1995) and hyoid/tongue retraction.

Quantitative analysis

In all species examined, the proportion of the muscles involved in jaw movements was always greater than the proportion of the muscles acting on the tongue and hyoid, both in terms of volume and PCSA

(Fig. 11, 12, left column). Although no clear pattern emerged, the aquatic *Typlonectes spp.* had the proportionately largest hyoid muscles among caecilians in terms of PCSA (Fig. 12, left column).

The comparison of the MIHP versus the three adductors showed that the MIHP by itself contributed more to the total PCSA and total volume than the sum of the adductors except in *R. bivittatum*. In *R. bivittatum* the volume and PCSA of the adductors were proportionally far greater than in the other species, in which the MIHP was preponderant (Fig. 11, 12, mid column).

Additionally, the contribution of the MPt and MLQ to the total volume and PCSA of the muscles included in our study was notably high for *R. bivittatum, I. kohtaoensis* and *Typhlonectes sp.* (Fig. 11, 12, right column) suggesting an important functional role in these species.

Discussion

Muscular anatomy

Our observations largely confirm or extend previous descriptions of adult caecilian head musculature (Bemis *et al*., 1983; Nussbaum, 1977; Nussbaum, 1983; Wake, 1986; Wilkinson and Nussbaum, 1997). Our results also highlight the singularity of the head musculature of the early-diverging rhinatrematids, represented here by *R. bivittatum,* as first reported by Nussbaum (1977). The main differences found among the species examined in this study lie in the morphology of the *m. adductores mandibulae* and the *m. interhyoideus*. Indeed, in all species except *R. bivittatum*—including even the zygokrotaphic *G. seraphini, T. natans and T. compressicauda*—the *m. adductores mandibulae* consist of three short muscular bundles (MAMA, MAML and MAMI) confined to the adductor chamber. Note, however, that a true MAMI, reported as absent by Parker (1941), was observed in *S. thomense*. In *R. bivittatum*, the MAML consists of three muscular bundles, the middle one of which is extremely large and has a central tendon. Moreover, the adductor complex in *R. bivittatum* extends dorsally, through the temporal fossa, to gain origin from the dorsal midline of the skull. Additionally, the MIHP of *R. bivittatum* has no tendon, whereas a tendon was found in the MIHP of all the other species included in our study. The MIHP of *R. bivittatum* is also small and ventrally positioned, whereas this muscle is large and caudally elongated in most species. As such, *R. bivittatum* likely represents the ancestral morphology with the traditional adductors functioning as the main jaw closers. *Ichthyophis kohtaoensis* shows a transitional morphology towards the anatomically derived caecilians. Indeed, *I. kohtaoensis* has a similar muscle architecture as other caecilians, but still possesses a relatively small and almost parallel-fibred MIHP. As previously observed (Wilkinson and Nussbaum, 1999), from *H. squalostoma* to *D. mexicanus*, all the teresomatan caecilians included in our study have relatively small adductors, and a comparatively large, caudally elongated *m. interhyoideus posterior*.

Based on developmental studies, Kleinteich and Haas (2007) confirmed the presence of the *m. pterygoideus* and m*. levator quadrati* in caecilians. Our results show that the *m. pterygoideus* is present in all species examined, and even consists of two distinct muscular bundles in *I. kohtaoensis* and *R. bivittatum*. Although globally horizontal, the fibre orientation of the MPt is quite complex as this muscle is quite variable in size and sometimes wraps around the pseudoangular, the *processus internus*, and also the stapes and *os basale* in *Typhlonectes*. The small *m. levator quadrati* was observed in all taxa except *Typhlonectes* and *R. bivittatum*. These results confirm a previous description of the Typhlonectidae in which no MLQ was found in *Typhlonectes* (Wilkinson and Nussbaum, 1997). However, according to the description of Nussbaum (1977), a MLQ is present in Rhinatrematidae. Yet, no MLQ was observed in dissections or µCT scans of *R. bivittatum*. However, the small size of the specimens, and the muscles, does not allow us to conclude with certainty the absence of the MLQ in *R. bivittatum*.

In terms of architecture, the subset of muscles responsible for hyoid and tongue movements investigated here are relatively similar for all the species examined and also similar to previous morphological descriptions (e.g. Nussbaum, 1977; Nussbaum, 1983; Wilkinson and Nussbaum, 1997). However, an additional *m. intermandibularis posterior* was found in *H. squalostoma* and in *G. seraphini*.

Muscular volume and PCSA

Our results highlight some interesting interspecific differences in the relative proportions of certain functional groups of muscles in terms of their volumes and PCSAs. Although volume and PCSA show similar trends, the latter includes more parameters, such as fibre length and pennation angle (see materials and methods), and is a good proxy of intrinsic muscle force output. The comparison between jaw muscles (MAMA, MAML, MAMI, MDM, MIHP, MPt and MLQ) and hyoid muscles (MGG, MGH, MRC, MIM and MIH) shows that the proportion of jaw muscles is always higher than that of hyoid muscles. In terms of PCSA, the aquatic *Typhlonectes* has a higher proportion of hyoid muscles than any other caecilians, and as such, more powerful hyoid muscles, likely important during buccal pumping (see Wilkinson and Nussbaum ,1997) and possibly also in suction feeding (O'Reilly, 2000). The inclusion of other aquatic caecilians such as *Potamotyphlus* or the unique *Atretochoana eiselti* (Wilkinson and Nussbaum, 1997) would be important to be able to definitively link this observation to the aquatic lifestyle of this taxon.

The comparison between the traditional adductors (MAMA, MAML and MAMI) and the unique *m. interhyoideus posterior* shows that for both volume and PCSA, the contribution of the adductors is much higher in *R. bivittatum* than in any other caecilian. Note that, to a lesser extent, the PCSA of the

adductors is also higher in *I. kohtaoensis*. These results confirm the hypotheses about the muscular proportions of these two muscular groups formulated by Nussbaum (1983). This means that in the early-diverging *R. bivittatum*, the traditional adductor-powered jaw-closing mechanism is more developed than the *m. interhyoideus posterior*. Again, *I. kohtaoensis* shows a transitional morphology towards the organization of more phylogenetically derived caecilians (Jetz and Pyron, 2018; Fig. S1). Indeed, in this species the maximal force that can be produced by the MIHP is already greater than the force produced by the adductors, but less so than in other species.

Finally, the global contribution of the functional groups highlights the variation in contribution to both volume and PCSA of the muscles involved in stability and kinetics of the skull, the *m. levator quadrati* and *m. pterygoideus*. These muscles are larger in the early-diverging *R. bivittatum* and *I. kohtaoensis*, but also in the aquatic *Typhlonectes,* suggesting important functional roles in these taxa.

Functional and evolutionary implications

As far as it is known, all caecilians have an at least partly fossorial lifestyle with the possible exception of some highly derived aquatic species such as the giant lungless *Atretochoana eiselti*. As head-first burrowing imposes significant constraints on the cranial system (O'Reilly, 2000; Wake, 1993), and as the costs of burrowing increase exponentially with increasing body diameter (Gans, 1968; Navas and Antoniazzi, 2004), caecilians developed a unique jaw-closing system involving the large and posteriorly placed *m. interhyoideus posterior* (Bemis *et al*., 1983; Nussbaum, 1983). This caudally elongated pennate-fibred muscle is positioned in such a way that its physiological cross section can be increased without a corresponding increase in head diameter (Bemis *et al*., 1983; Nussbaum, 1983). All caecilians included in our study possess this dual jaw-closing mechanism, but as previously observed (Nussbaum, 1977), *R. bivittatum* is morphologically quite different from the other species. Indeed, *R. bivittatum*, phylogenetically the most early-diverging species included in our dataset, invests more into the traditional lateral jaw adductors (MAMA, MAML and MAMI) than in the *m. interhyoideus posterior*. Moreover, whereas its MIHP does not bear any tendon, the MAML has a relatively robust tendon. Compared to parallel-fibred and tendonless muscles, bipennate muscles composed of shorter fibres produce more force to the detriment of velocity (Nussbaum, 1983; Summers and Wake, 2005). As a result (see also Lowie *et al*., 2022), *R. bivittatum* likely generates more of its bite force using powerful adductors rather than the MIHP. Indeed, although models show that a long retroarticular process coupled with a large MIHP increases bite force (Summers and Wake, 2005), bite force also covaries with the volume and the PCSA of the adductors (Lowie *et al*., 2022). On the other hand, large adductors, which take their origins from the very top on the cranium, could negatively impact burrowing performance. In this context, it is perhaps significant to note that *R. bivittatum* is more

surface active than many other caecilians, and as such, may not impacted as much by an increase in head diameter.

As also discussed by Nussbaum (1983), *Ichthyophis kohtaoensis,* also suggested as more surface active than other dedicated burrowers (Kupfer *et al.*, 2005; Ramaswamii, 1941; Wollenberg and Measey, 2009), represents an intermediate phylogenetic and functional stage between the more ancestral morphology of *R. bivittatum* and the more derived morphology of teresomatan caecilians (Fig. S1). Its retroarticular process is larger, and the MIHP has a tendon but its fibres are only slightly pennate. Its adductors are tendonless, parallel-fibred and confined to the adductor chamber. In the other terrestrial species examined, the MIHP has become larger and more caudally elongated, while the adductors remain confined to the temporal region, not extending to the top of the cranium, even in the zygokrotaphic *Typlonectes* and *G. seraphini*. Globally, the muscular architecture of the jaw muscles remains similar throughout the Teresomata. As observed in Lowie *et al*. (2022), a gradient does exist, however, with species gradually transitioning from having large adductors and a small MIHP associated with a small retroarticular process, to small and parallel-fibred adductors confined in the adductor chamber and large MIHP associated with longer retroarticular process.

Caecilians are known to maintain body turgor through their high pleuroperitoneal pressure, which plays a role in their mechanism of hydrostatic locomotion (Carrier and Wake, 1995; O'Reilly *et al*., 1997). Additionally, the aquatic *Typhlonectes* not only possesses a significantly developed second lung, but its lungs are also elongated compared to the other species included in our study (Wilkinson and Nussbaum, 1997). As a result, although all caecilians rely on buccal pumping to maintain a certain pleuroperitoneal pressure, aquatic species may rely more on ventilatory capacities and buccal pumping than terrestrial species. In accordance with the observations of Wilkinson and Nussbaum (1997), our results show that although the hyoid musculature is well developed in all caecilians examined, its importance is greater in the aquatic *Typhlonectes*. Moreover, while terrestrial caecilians use jaw prehension to capture prey, aquatic species also use compensatory suction feeding (Herrel *et al*., 2019; O'Reilly, 2000), and as such, strong hyoid musculature may be beneficial to move the hyoid and the buccal floor to generate the negative pressures needed for suction feeding.

Although the exact roles of the *m. levator quadrati* and the *m. pterygoideus* remain to be confirmed by functional and/or modeling studies, these muscles are unique to caecilians (Kleinteich and Haas, 2007) among amphibians and show some morphological differences among the species examined. A true MLQ was not found in *R. bivittatum* or *Typhlonectes*. Although this confirms a previous study that did not observe a MLQ in *Typhlonectes* (Wilkinson and Nussbaum, 1997), Nussbaum (1977) reported a MLQ in *Rhinatrema*. In Scolecomorphidae, the MLQ is also absent (Müller *et al*., 2009). As the MLQ

originates from the *os basale* and inserts on the pterygoid process of the quadrate, it is likely involved in the mobility of the quadrate (streptostyly). As highlighted by Summers and Wake (2005), an increase in mobility of the cheek region may lead to an increase in bite force. Species lacking a MLQ could then be expected to feed more on soft-bodied prey. Additionally, the MLQ could play a role in jaw stabilization during feeding (Bemis *et al*., 1983). As caecilians also use rotational feeding (Measey and Herrel, 2006), the presence of a MLQ could help to prevent the dislocation of the quadrate complex during rotational feeding. Similarly, the *m. pterygoideus* also inserts onto the pterygoid process, and as such, could also play a role in stabilizing the jaws during rotational feeding.

In the representatives of the two most early-diverging families included in our study, *i.e. R. bivittatum* and *I. kohtaoensis*, a *m. pterygoideus internus* is also present. According to Müller *et al*. (2009), this muscle is also present in Scolecomorphidae (adults and foetuses). Similar to the MLQ, the MPt may play a role in cranial kinesis although this remains to be tested. The presence of two bundles of the MPt in the three most early-diverging lineages suggests that this may be an ancestral trait. Interestingly, the MPt is also well developed in the aquatic species included in our study suggesting that its presence in these animals may be functional and not merely the persistence of an ancestral trait. Indeed, the MPt may contribute to bite force generation at large gape and as such may be important in closing the mouth rapidly in suction feeders. Yet, this remains to be tested. To better understand the functional roles of the MLQ and MPt further analyses including electromyographical recordings during buccal pumping and feeding to better understand the function of both muscles (Herrel *et al*., 2019). Additionally, histological studies could be performed on the small hyobranchial muscles to morphologically and functionally compare them across caecilians.

Conclusion

The organization of the head musculature is relatively consistent across extant caecilians. However, the early-diverging *R. bivittatum* relies primarily on the 'traditional' amphibian jaw-closing mechanism involving the *m. adductores mandibulae*, whereas derived caecilians transitioned toward the use of a novel dual jaw-closing mechanisms involving the *m. interhyoideus posterior* together with the *m. adductores mandibulae*. Additionally, the aquatic *Typhlonectes* show a greater investment in hyoid musculature than terrestrial caecilians, which is likely related to its increased reliance on buccal pumping and possibly also to suction feeding. The *m. levator quadrati and m. pterygoideus* are quite variable in morphology across the caecilians examined. Further studies are needed to fully interpret their function and evolution across Gymnophiona. Our data provide the required quantitative data to facilitate the generation of accurate biomechanical models to test additional functional hypotheses.

Acknowledgements

We thank I. Josipovic and the people at Centre for X-Ray Tomography at Ghent University for their help with CT scanning. We thank the Natural History Museum (London), Museum of Zoology (University of Michigan), the Amphibian & Reptile Diversity Research Centre (University of Texas Arlington), the Zoological Museum (Hamburg), A. Kupfer and the Staatliches Museum für Naturkunde Stuttgart and all the curators in these institutions for the loan of some key specimens. A.L. thanks M. H. Wake for the gift of *Dermophis* specimens and B. DuBois for his help in generating the two interactive 3D models.

Competing interests

The authors declare no competing or financial interests.

Author contributions

A. L. A. H. and D. A. designed the study; A. L., A. H., B. DK., J. M., J. O'R., M. W., N. J. K. and P. G. acquired data; A.L. performed the analyses; A. L. drafted the manuscript; all authors contributed to the final manuscript, read and approved it.

Funding

This study was supported by the Research Foundation, Flanders (Fonds Wetenschappelijk Onderzoek, grant 11D5819N), a Tournesol travel grant, the Royal Belgian Zoological Society and a European Union Marie Curie Fellowship (HPMF-CT-2001-01407), field work and visiting fellowship of the Fonds Wetenschappelijk Onderzoek, Flanders, Belgium (FWO-Vl) to J. M. The special research fund of Ghent University (BOF-UGent) is acknowledged for financial support of the UGCT Centre of Expertise (BOF.EXP.2017.0007).

Data availability statement

The data that support the findings of this study are available from the corresponding author upon reasonable request

References

Bardua, C., Wilkinson, M., Gower, D. J., Sherratt, E. and Goswami, A. (2019). Morphological evolution and modularity of the caecilian skull. *BMC Evol. Biol.* **19**, 1–24.

Bemis, W. E., Schwenk, K. and Wake, M. H. (1983). Morphology and function of the feeding apparatus in *Dermophis mexicanus* (Amphibia: Gymnophiona). *Zool. J. Linn. Soc.* **77**, 75–96.

Carrier, D. R. and Wake, M. H. (1995). Mechanism of lung ventilation in the caecilian *Dermophis*

562 *mexicanus*. *J. Morphol*. **226**, 289–295.

563 **Carroll, R. L.** (2007). The palaeozoic ancestry of salamanders , frogs and caecilians. *Zool. J. Linn. Soc.*
564 **150**, 1–140.

565 **Descamps, E., Sochacka, A., de Kegel, B., Loo, D. Van, Hoorebeke, L. and Adriaens, D.** (2014). Soft
566 tissue discrimination with contrast agents using micro-ct scanning. Belgian J. Zool. **144**, 20–40.

567 **Ducey, P. K., Formanowicz, D. R. J., Boyet, L., Mailloux, J. and Nussbaum, R. A.** (1993). Experimental
568 examination of burrowing behavior in caecilians (Amphibia: Gymnophiona): effects of soil
569 compaction on burrowing ability of four species. *Herpetologica* **49**, 450–457.

570 **Dunn, E.** (1942). The American caecilians. *Bull. Museum Comp. Zool.* **91**, 437–540.

571 **Gans, C.** (1968). Relative success of divergent pathways in amphisbaenian specialization. *Am. Nat.* **102**,
572 345–362.

573 **Gans, C.** (1974). *Biomechanics. An approach to vertebrate biology*. Philadelphia, PA, USA: J.B.
574 Lippincott Company.

575 **Gignac, P. M., Kley, N. J., Clarke, J. A., Colbert, M. W., Morhardt, A. C., Cerio, D., Cost, I. N., Cox, P.**
576 **G., Daza, J. D., Early, *et al.*** (2016). Diffusible iodine-based contrast-enhanced computed
577 tomography (diceCT): an emerging tool for rapid, high-resolution, 3-D imaging of metazoan soft
578 tissues. *J. Anat.* **228**, 889–909.

579 **Haas, A**. (2001). Mandibular arch musculature of anuran tadpoles, with comments on homologies of
580 amphibian jaw muscles. *J. Morphol*. **247**, 1–33.

581 **Herrel, A. and Measey, G. J.** (2010). The kinematics of locomotion in caecilians: effects of substrate
582 and body shape. *J. Exp. Zool. Part A Ecol. Genet. Physiol.* **313A**, 301–309.

583 **Herrel, A., Reilly, J. C. O., Fabre, A., Bardua, C., Lowie, A., Boistel, R. and Gorb, S. N.** (2019). Feeding
584 in amphibians: evolutionary transformations and phenotypic diversity as drivers of feeding
585 system diversity. In *Feeding in Vertebrates* (ed. Bels, V. and Whishaw, I. Q.), pp. 431–467. Cham,
586 Switzerland: Springer Nature.

587 **Jetz, W., Pyron, R. A.** (2018). The interplay of past diversification and evolutionary isolation with
588 present imperilment across the amphibian tree of life. *Nat. Ecol. Evol.* **2**, 850–858.

589 **Kleinteich, T. and Haas, A.** (2007). Cranial musculature in the larva of the caecilian, *Ichthyophis*
590 *kohtaoensis* (Lissamphibia: Gymnophiona). *J. Morphol.* **268**, 74–88.

591 **Kleinteich, T. and Haas, A.** (2011). The hyal and ventral branchial muscles in caecilian and salamander
592 larvae: homologies and evolution. *J. Morphol*. **272**, 598–613.

Kleinteich, T., Haas, A. and Summers, A. P. (2008). Caecilian jaw-closing mechanics: integrating two muscle systems. *J. R. Soc. Interface* **5**, 1491–1504.

Kleinteich, T., Maddin, H. C., Herzen, J., Beckmann, F. and Summers, A. P. (2012). Is solid always best? Cranial performance in solid and fenestrated caecilian skulls. *J. Exp. Biol.* **215**, 833–844.

Kupfer, A., Nabhitabhata, J., Himstedt, W. (2005). Life history of amphibians in the seasonal tropics: habitat, community and population ecology of a caecilian (genus *Ichthyophis*). *J. Zool.* **266**, 237–247.

Kupfer, A. (2009). Sexual size dimorphism in caecilian amphibians: analysis, review and directions for future research. *Zoology* **112**, 362–369.

Lowie, A., De Kegel, B., Wilkinson, M., Measey, J., O'Reilly, J. C., Kley, N. J., Gaucher, P., Brecko, J., Kleinteich, T., Van Hoorebeke, L., Herrel, A. and Adriaens D. (2021). Under pressure: the relationship between cranial shape and burrowing force in caecilians (Gymnophiona). *J. Exp. Biol.* **224**, jeb242964.

Lowie, A., De Kegel, B., Wilkinson, M., Measey, J., O'Reilly, J. C., Kley, N. J., Gaucher, P., Brecko, J., Kleinteich, T., Adriaens, D., and Herrel A. (2022). The relationship between head shape, head musculature and bite force in caecilians (Amphibia: Gymnophiona). *J. Exp. Biol*. **225**, jeb243599.

Maciel, A. O., Gomes, J. O., Costa, J. C. L., Andrade, G. V. (2012). Diet, microhabitat use, and an analysis of sexual dimorphism in *Caecilia gracilis* (Amphibia: Gymnophiona: Caeciliidae) from a riparian forest in the Brazilian Cerrado. *J. Herpetol.* **46**, 47–50.

Masschaele, B., Dierick, M., Van Loo, D., Boone, M. N., Brabant, L., Pauwels, E., Cnudde, V. and Van Hoorebeke, L. (2013). HECTOR: A 240kV micro-CT setup optimized for research. *J. Phys. Conf. Ser.* **463**, 012012.

Measey, G. J. and Herrel, A. (2006). Rotational feeding in caecilians: putting a spin on the evolution of cranial design. *Biol. Lett.* **2**, 485–487.

Mendez, J. and Keys, A. (1960). Density and composition of mammalian muscle. *Metabolism* **9**, 184–188.

Müller, H., Wilkinson, M., Loader, S. P., Wirkner, C. S. and Gower, D. J. (2009). Morphology and function of the head in foetal and juvenile *Scolecomorphus kirkii* (Amphibia: Gymnophiona: Scolecomorphidae). *Biol. J. Linn. Soc*. **96**, 491–504.

Navas C. A. and Antoniazzi M. M. (2004). Morphological and physiological specialization for digging in amphisbaenians, an ancient lineage of fossorial vertebrates. *J. Exp. Biol.* **207**, 2433–2441.

Nussbaum, R. A. (1977). Rhinatrematidae: a new family of caecilians (Amphibia: Gymnophiona). *Occas. Pap. Museum Zool*. **682**, 1–30.

Nussbaum, R. A. (1983). The evolution of a unique dual jaw-closing mechanism in caecilians (Amphibia: Gymnophiona) and its bearing on caecilian ancestry. *J. Zool., Lond.* **199**, 545–554.

Nussbaum, R. A. and Pfrender, M.E. (1998). Revision of the African caecilian genus *Schistometopum* Parker (Amphibia: Gymnophiona: Caeciliidae). *Misc. Publ. Museum Zool. Univ. Michigan* **187**, 1–32.

O'Reilly, J. C. (2000). Feeding in caecilians. In *Feeding: Form, Function, and Evolution in Tetrapod Vertebrates* (ed. Schwenk, K.), pp. 149–166. San Diego, CA, USA: Academic Press.

O'Reilly, J. C., Ritter, D. A. and Carrier, D. R. (1997). Hydrostatic locomotion in a limbless tetrapod. *Nature* **386**, 269–272.

Parker, H. W. (1941). The caecilians of the Seychelles. *Ann. Mag. Nat. Hist*. Ser. II. **7**, 1–17.

Ramaswami, L. S. (1941). Some aspects of the cranial morphology of *Uraeotyphlus narayani* Seshachar (Apoda). *Rec. indian museum* **43**, 143–207.

Sherratt, E., Gower, D. J., Klingenberg, C. P. and Wilkinson, M. (2014). Evolution of cranial shape in caecilians (Amphibia: Gymnophiona). *Evol. Biol.* **41**, 528–545.

Summers, A. P. and Wake, M. H. (2005). The retroarticular process, streptostyly and the caecilian jaw closing system. *Zoology* **108**, 307–315.

Taylor, E. H. (1969). Skulls of Gymnophiona and their significance in the taxonomy of the group. *Univ. Kansas Sci. Bull.* **48**, 585–687.

Theska, T., Wilkinson, M., Gower, D. J. and Mueller, H. (2018). Musculoskeletal development of the Central African caecilian *Idiocranium russeli* (Amphibia: Gymnophiona: Indotyphlidae) and its bearing on the re-evolution of larvae in caecilian amphibians. *Zoomorphology* **138**, 137–158.

Verdade, V., Schiesari, L. and Bertoluci, J. (2000). Diet of juvenile aquatic caecilians, *Typhlonectes compressicauda*. *J. Herpetol.* **34,** 291–293.

Wake, M. H. (1986). The morphology of *Idiocranium russeli* (Amphibia: Gymnophiona), with comments on miniaturization through heterechrony. *J. Morphol.* **189**, 1–16.

Wake, M. H. (1993). The skull as a locomotor organ. In *The skull: functional and evolutionary mechanisms* (ed. Hanken, J. and Hall, B. K.), pp. 197–240. Chicago, IL, USA: University of Chicago Press.

Wake, M. H. and Hanken, J. (1982). Development of the skull of *Dermophis mexicanus* (Amphibia:

Gymnophiona), with comments on skull kinesis and amphibian relationships. *J. Morphol.* **173**, 203–223.

Wiedersheim, R. (1879) Die Anatomie der Gymnophionen. Jena: Gustav Fischer.

Wilkinson, M. (2012). Caecilians. Curr. Biol. 22, 668–669.

Wilkinson, M. and Nussbaum, R. A. (1997). Comparative morphology and evolution of the lungless caecilian *Atretochoana eiselti* (Taylor) (Amphibia: Gymnophiona: Typhlonectidae). *Biol. J. Linn. Soc.* **62**, 39–109.

Wollenberg, K.C. and Measey, G.J. (2009). Why colour in subterranean vertebrates ? Exploring the evolution of colour patterns in caecilian amphibians. *J. Evol. Biol*. **22**, 1046–1056.

Tables

Table 1. Details of specimens used in this study with family, species names and number of individuals (n) for each data set.

Family	Species	n Dissections	n Stained µCT
Rhinatrematidae	*Rhinatrema bivittatum*	4	1
Ichthyophiidae	*Ichthyophis kohtaoensis*	2	1
Herpelidae	*Herpele squalostoma*	5	1
	Boulengerula taitanus	10	1
	Boulengerula fischeri	4	1
Caeciliidae	*Caecilia tentaculata*	0	1
	Caecilia museugoeldi	0	1
Typhlonectidae	*Typhlonectes compressicauda*	2	0
	Typhlonectes natans	0	1
Siphonopidae	*Microcaecilia unicolor*	1	1
Dermophiidae	*Geotrypetes seraphini*	7	1
	Dermophis mexicanus	2	1
	Schistometopum thomense	3	1

Legends

Figure 1. Three-dimensional (3D) overview of the muscles included in this study. Visualized on a *Dermophis mexicanus*. A: complete skull and musculature; B: muscles and the quadrato-squamosal are removed. Hy: Hyoid, MAMA: *m. adductor mandibulae articularis,* MAML: *m. adductor mandibulae longus,* MDM: m*. depressor mandibulae*, MGH: *m. geniohyoideus*, MIHA: *m. interhyoideus anterior*, MIHP: *m. interhyoideus posterior*, MIM: *m. intermandibularis*, MLQ: *m. levator quadrati*, MPt: *m. pterygoideus,* MRC: *m. rectus cervicis,* Sq: squamosal. The *m. adductor mandibulae articularis* and the *m. genioglossus* respectively hidden behind the MAML and the mandible are not represented here. All images in right lateral view.

Figure 2. Three-dimensional (3D) visualization of the morphological variations observed in the *m. depressor mandibulae* (MDM) in caecilian amphibians. A: *Caecilia tentaculata*; B: *Dermophis mexicanus*; C: *Rhinatrema bivittatum* (light pink: MDM, dark pink: *m. adductor mandibulae longus* [MAML]); D: *Typhlonectes natans*. All images in right lateral view.

Figure 3. Three-dimensional (3D) visualization of the morphological variations observed in the *m. interhyoideus anterior* (MIHA; dark pink) and *m. interhyoideus posterior* (MIHP; light pink) in caecilian amphibians. A: *Caecilia tentaculata*; B: *Ichthyophis kohtaoensis*; C: *Rhinatrema bivittatum*. Note that the body of the *C. tentaculata* was bent during the scanning process, resulting in a ventral bending of the neck musculature, which is normally in line with the body. All images in right lateral view.

Figure 4. Three-dimensional (3D) visualization of the adductors and the *m. levator quadrati* in *Caecilia tentaculata*. A: complete skull showing the squamosal (Sq) covering the temporal region; B: squamosal bone removed to show the *m. adductor mandibulae longus* (MAML); C: MAML removed to show the m*. adductor mandibulae internus* (MAMI); D: MAMI removed to show the *m. levator quadrati* (MLQ); E: complete cranium removed to show the m*. adductor mandibulae articularis* (MAMA; dark pink) previously hidden deep to the quadrate bone. All images in right lateral view.

Figure 5. Three-dimensional (3D) visualization of the *m. adductor mandibulae longus* (MAML) in *Geotrypetes seraphini*. Image in right lateral view.

Figure 6. Three-dimensional (3D) visualization of the adductors in *Rhinatrema bivittatum*. A: the squamosal bone and the *m. adductor mandibulae articularis* (MAMA) were removed to visualize the *m. adductor mandibulae longus* (MAML) complex. Light pink: MAML with its white tendon, dark pink: small lateral bundle of MAML (MAML lat.); B: these two MAML bundles were removed to show the most medial muscle of the MAML complex (MAML med.); C: m*. adductor mandibulae internus* (MAMI) complex. Light pink: anterior portion of the MAMI (MAMI ant.), dark pink: posterior portion of the MAMI (MAMI post.). Both insert onto the white tendon; D: MAML and MAMI were removed, and transparency was applied to the squamosal bone to visualize the MAMA under the bone. All images in right lateral view.

Figure 7. Three-dimensional (3D) visualization of the *m. adductor mandibulae internus* (MAMI) in *Ichthyophis kohtaoensis*. Squamosal bone and *m. adductor mandibulae longus* were removed to visualize the MAMI. OB: *os basale*, Sp: Sphenetmoid. Image in right lateral view.

Figure 8. Three-dimensional (3D) visualization of the *m. pterygoideus* (MPt) in caecilian amphibians. A: *Caecilia tentaculata*; B: *Rhinatrema bivittatum*; C: *Rhinatrema bivittatum*, the MPt was removed,

and transparency was applied to the cranium to visualize the internal MPt (MPt int.) behind the pterygoid. All images in right medial view.

Figure 9. Three-dimensional (3D) visualization of the *m. intermandibularis* (MIM) in caecilian amphibians. A: *Caecilia tentaculata*; B: *Geotrypetes seraphini*, light pink: posterior MIM (MIM post.), dark pink: anterior MIM (MIM ant.). Images in ventral view.

Figure 10. Three-dimensional (3D) visualization of the hypoglossus muscles in *Caecilia tentaculata*. A: lingual view, light pink: *m. genioglossus* (MGG), dark pink: *m. geniohyoideus* (MGH) and *m. rectus cervicis* (MRC); B: ventral view, light pink: MGH, dark pink: MRC.

Figure 11. Graphs showing the muscular volume contribution across caecilian amphibians. Left: muscles involved in jaw movements (MAMA + MAML + MAMI + MIHP + MDM + MPt + MLQ) compared to the muscles involved in hyoid movements (MGG + MGH + MRC + MIM + MIH); Middle: jaw-adductors (MAMA + MAML + MAMI) compared to the *m. interhyoideus posterior*; Right: contribution of different functional groups across caecilian amphibians. Jaw-adductors (MAMA + MAML + MAMI); unique jaw closer (MIHP); jaw-stabilisers (MLQ + MPt); jaw-opener (MDM); hyoid muscles (MGG + MGH + MRC + MIM + MIH).

Figure 12. Graphs showing the muscular PCSA contribution across caecilian amphibians. Left: muscles involved in jaw movements (MAMA + MAML + MAMI + MIHP + MDM + MPt + MLQ) compared to the muscles involved in hyoid movements (MGG + MGH + MRC + MIM + MIH); Middle: jaw-adductors (MAMA + MAML + MAMI) compared to the *m. interhyoideus posterior*; Right: contribution of different functional groups across caecilian amphibians. Jaw-adductors (MAMA + MAML + MAMI); unique jaw closer (MIHP); jaw-stabilisers (MLQ + MPt); jaw-opener (MDM); hyoid muscles (MGG + MGH + MRC + MIM + MIH).

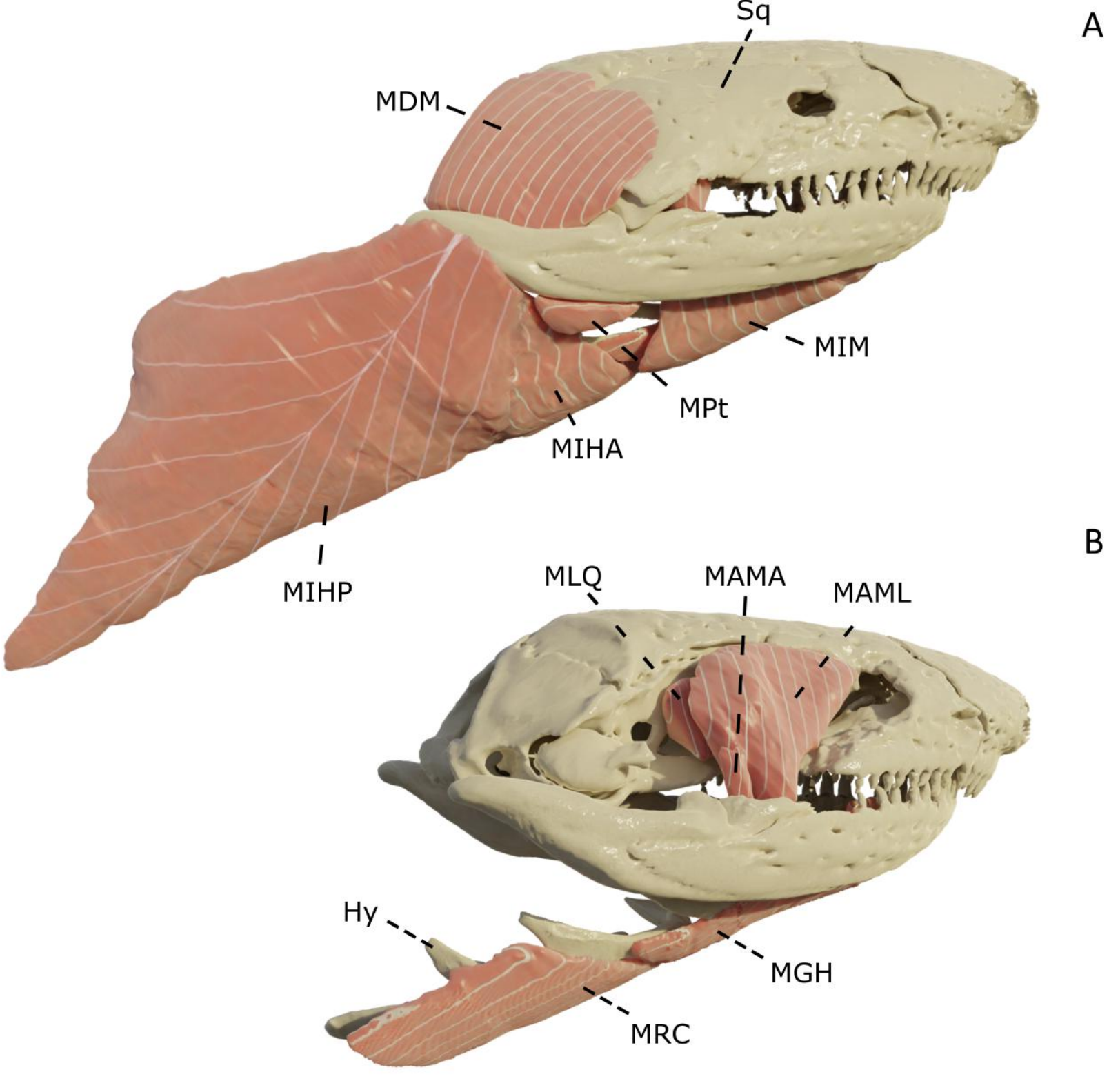
A
Sq
MDM
MIM
MPt
MIHA
MIHP
B
MLQ
MAMA
MAML
Hy
MGH
MRC

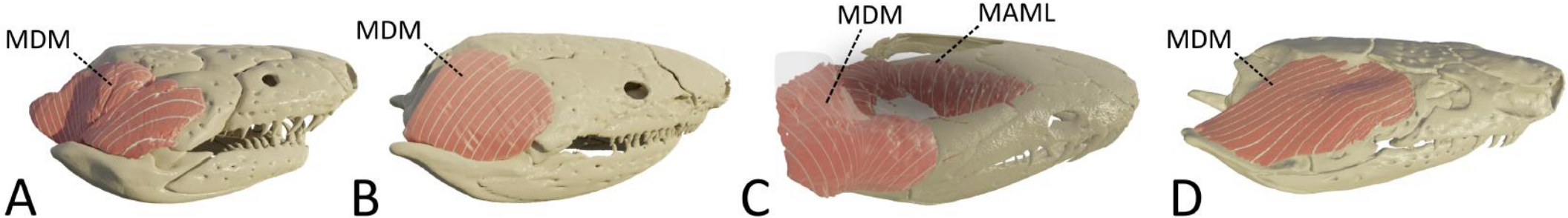
MDM
A
Caecilia tentaculata
MDM
B
Dermophis mexicanus
MDM
MAML
C
Rhinatrema bivittatum
MDM
D
Typhlonectes natans

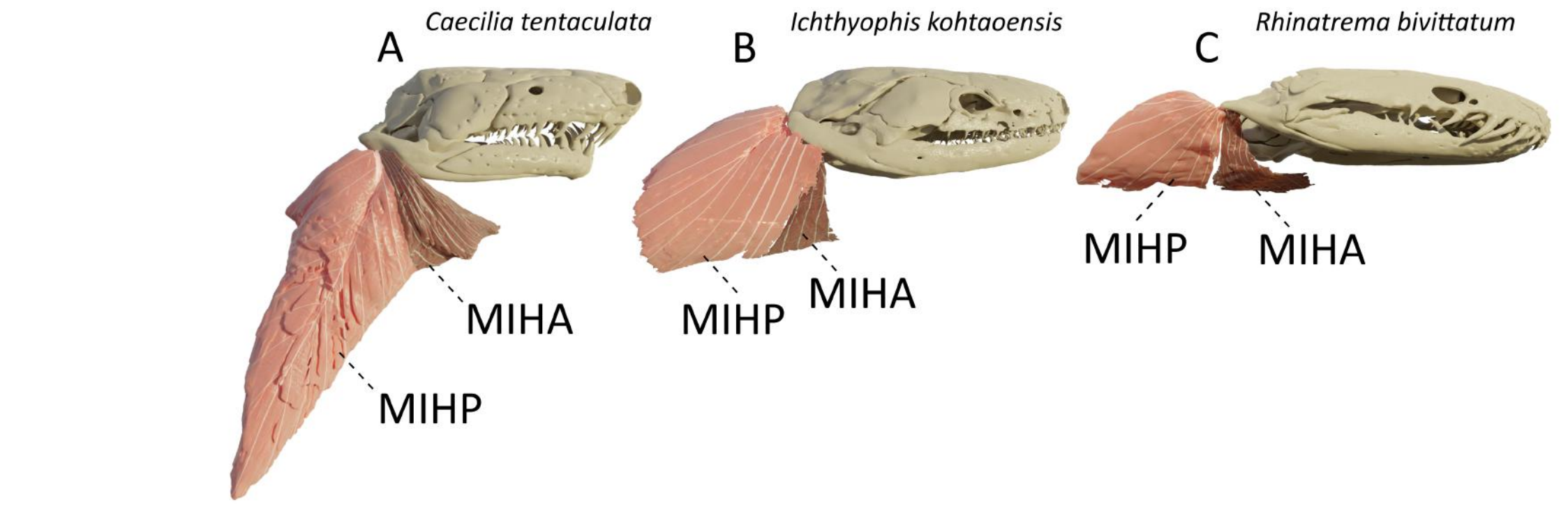
A
Caecilia tentaculata
MIHA
MIHP
B
Ichthyophis kohtaoensis
MIHP
MIHA
C
Rhinatrema bivittatum
MIHP
MIHA

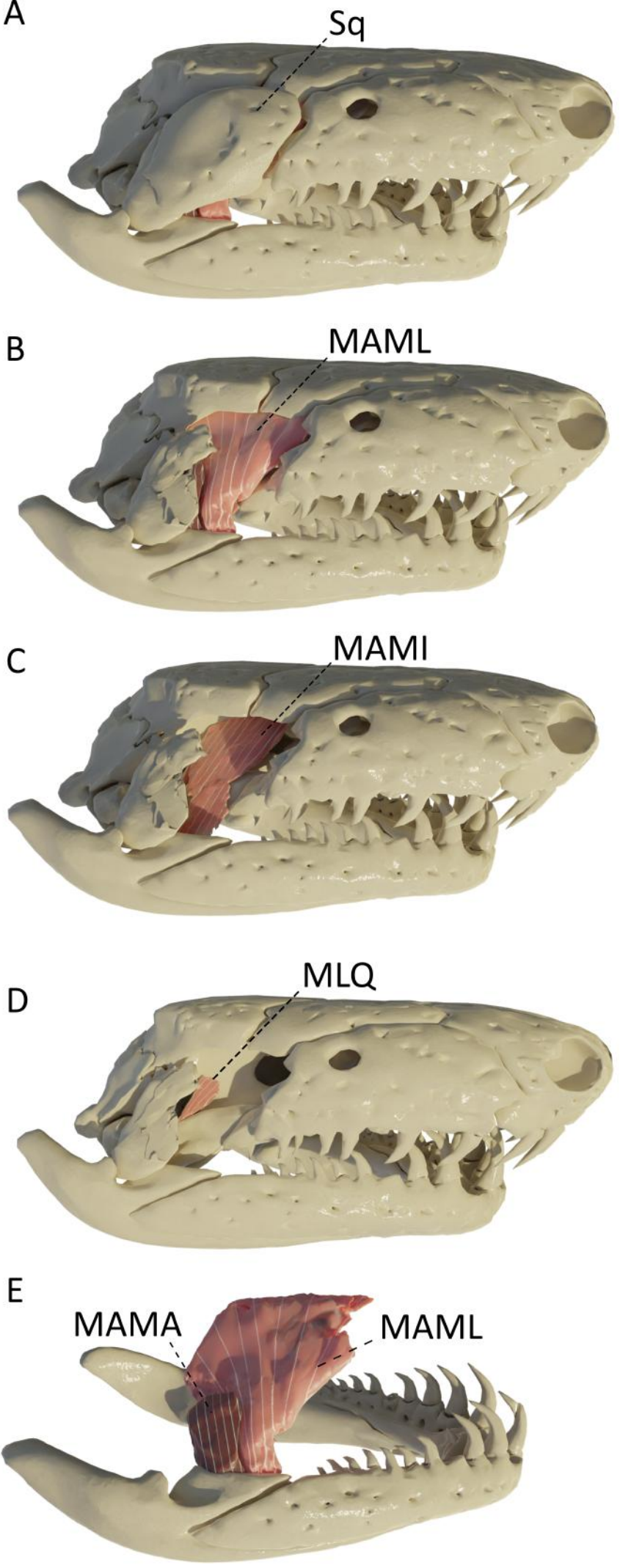
A
Sq
B
MAML
C
MAMI
D
MLQ
E
MAMA
MAML

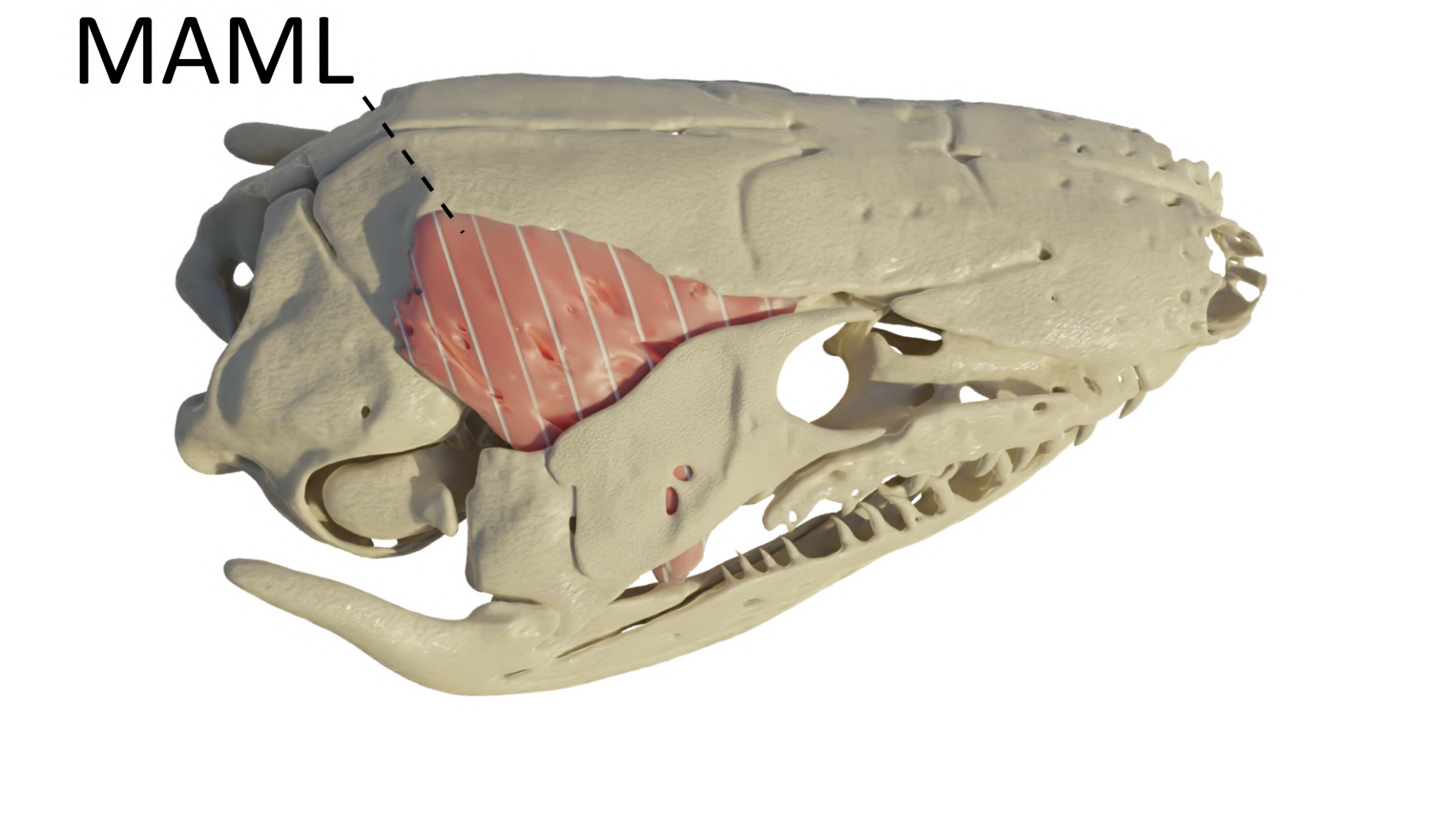
MAML

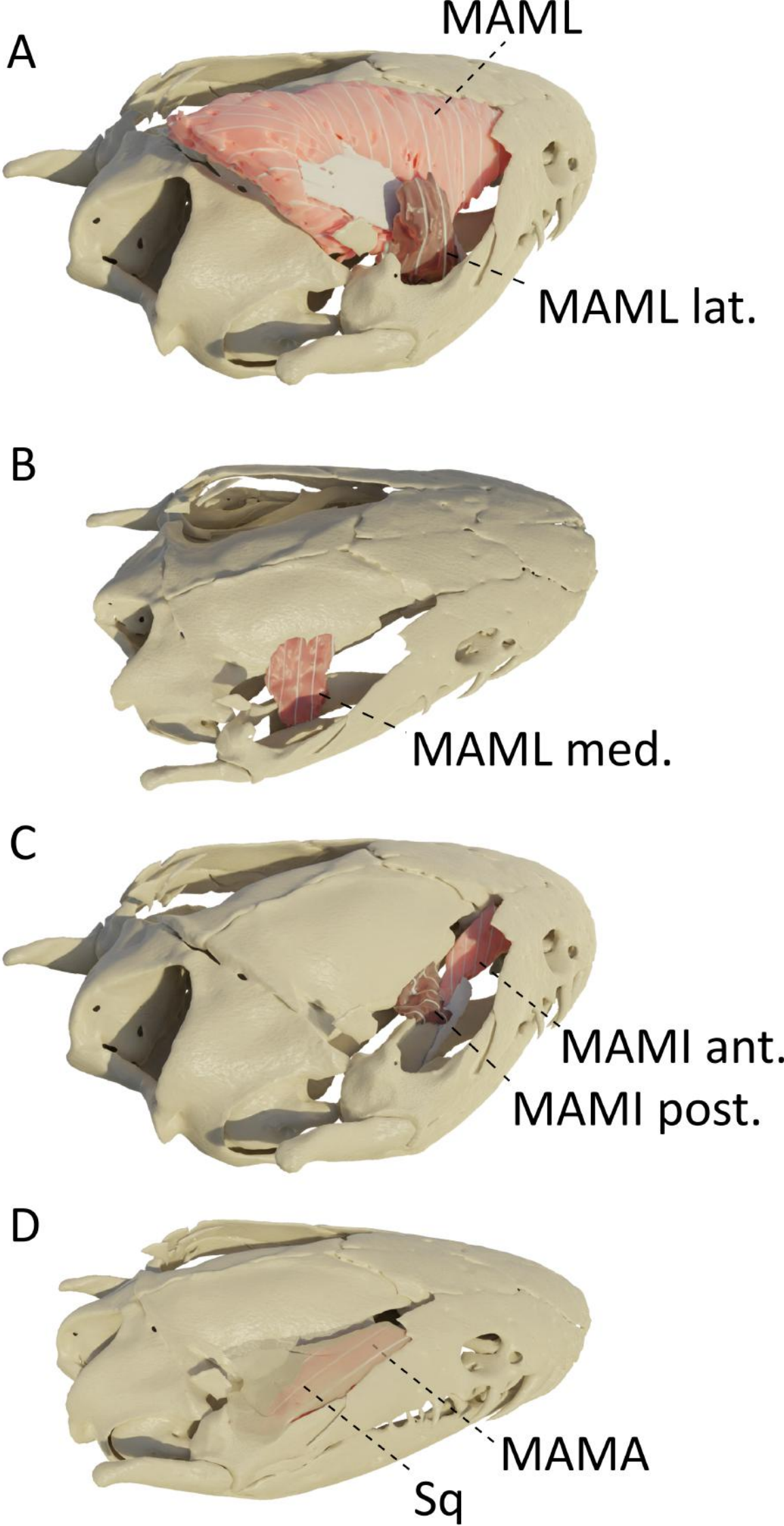
A
MAML
MAML lat.
B
MAML med.
C
MAMI ant.
MAMI post.
D
MAMA
Sq

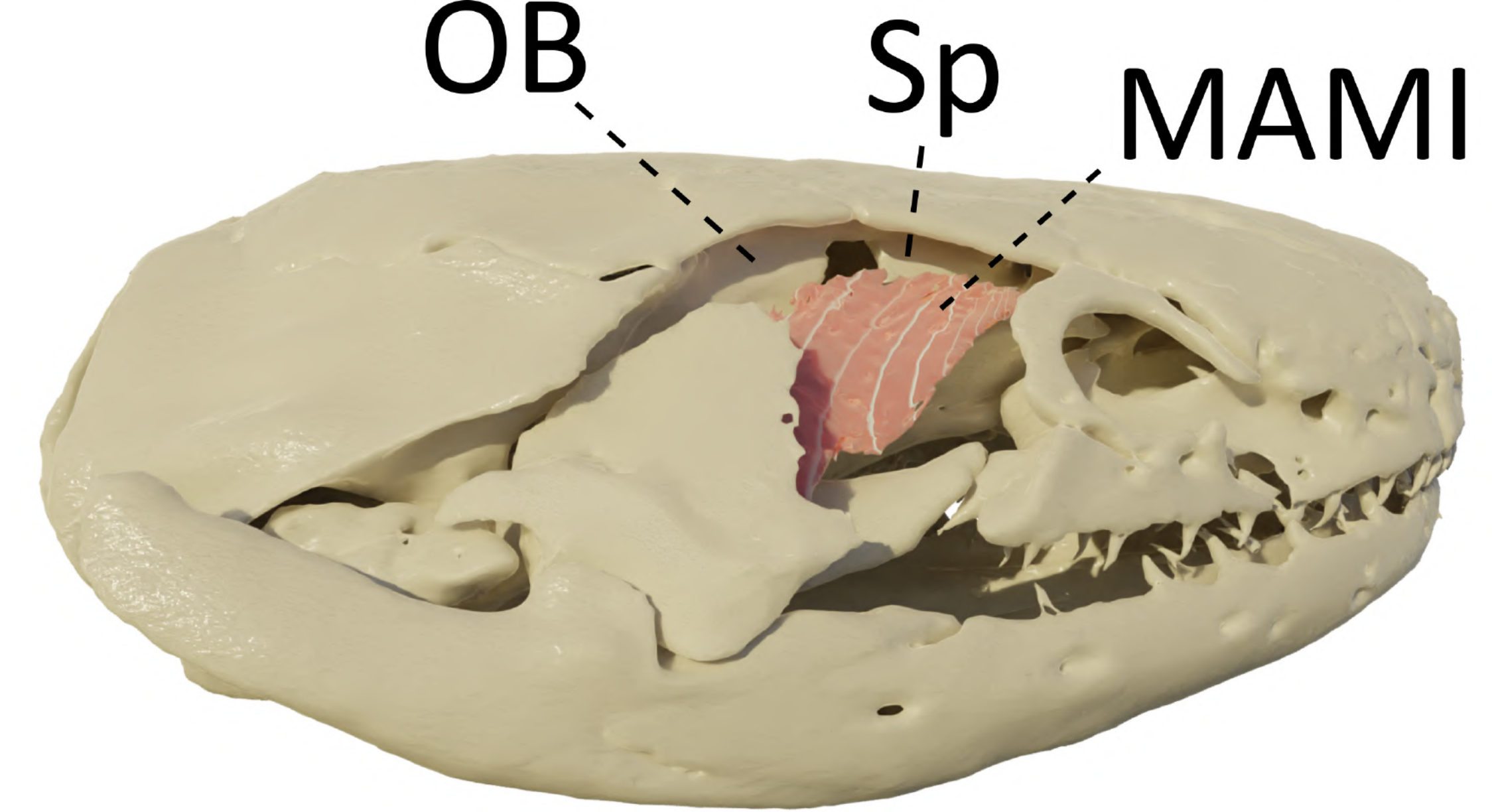
OB
Sp
MAMI

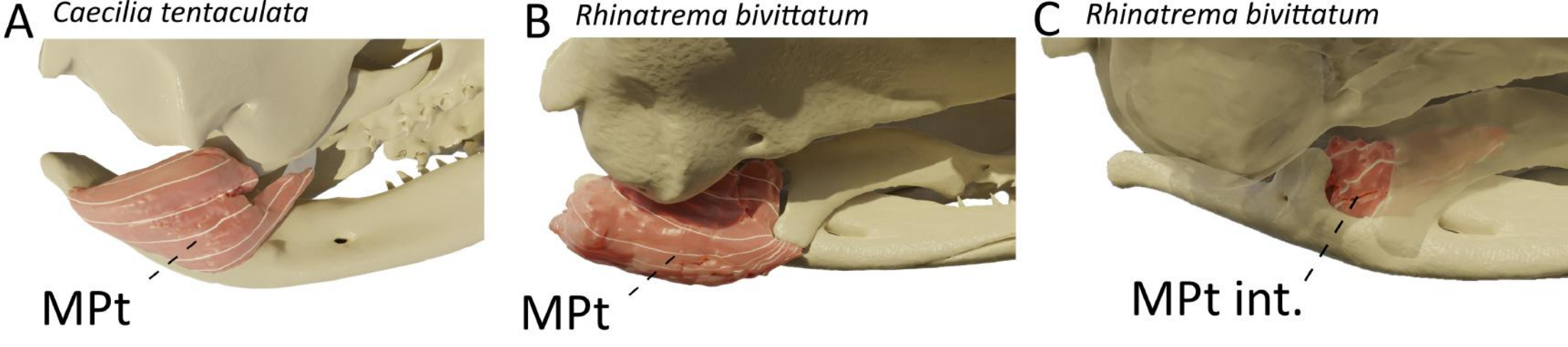
A
Caecilia tentaculata
MPt
B
Rhinatrema bivittatum
MPt
C
Rhinatrema bivittatum
MPt int.

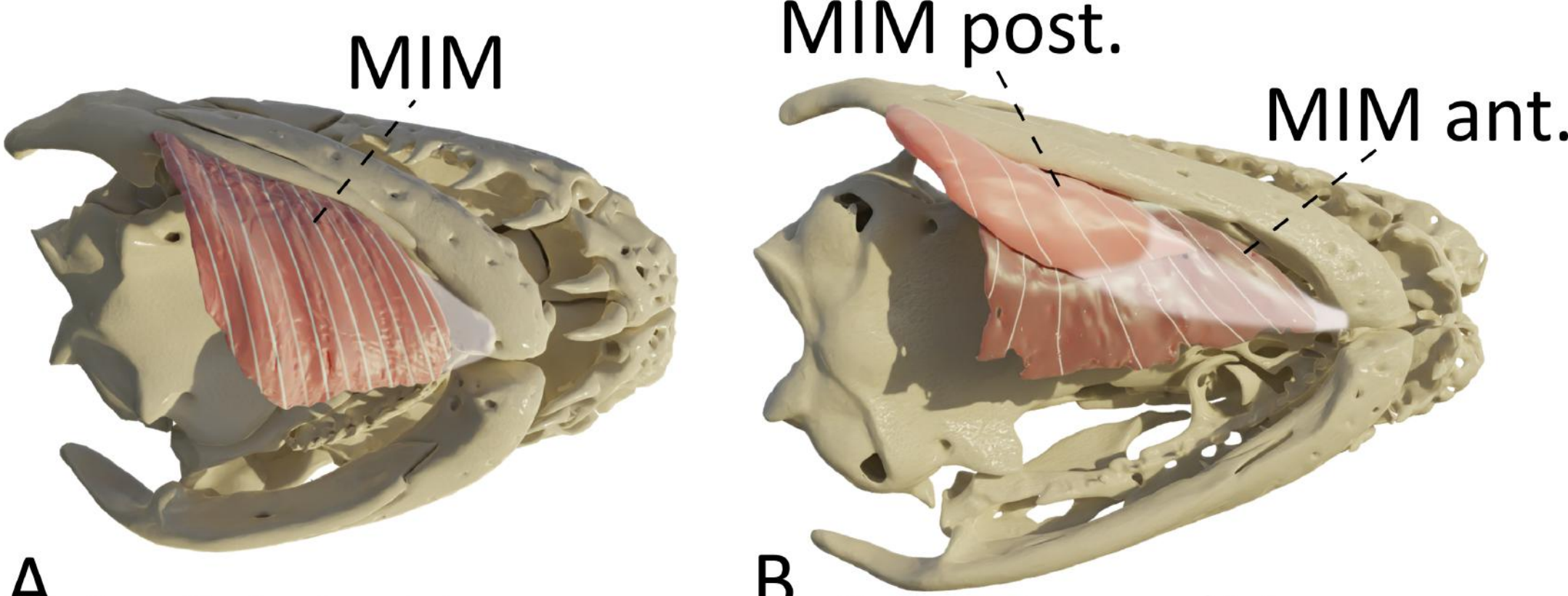
MIM
MIM post.
MIM ant.
A
Caecilia tentaculata
B
Geotrypetes seraphini

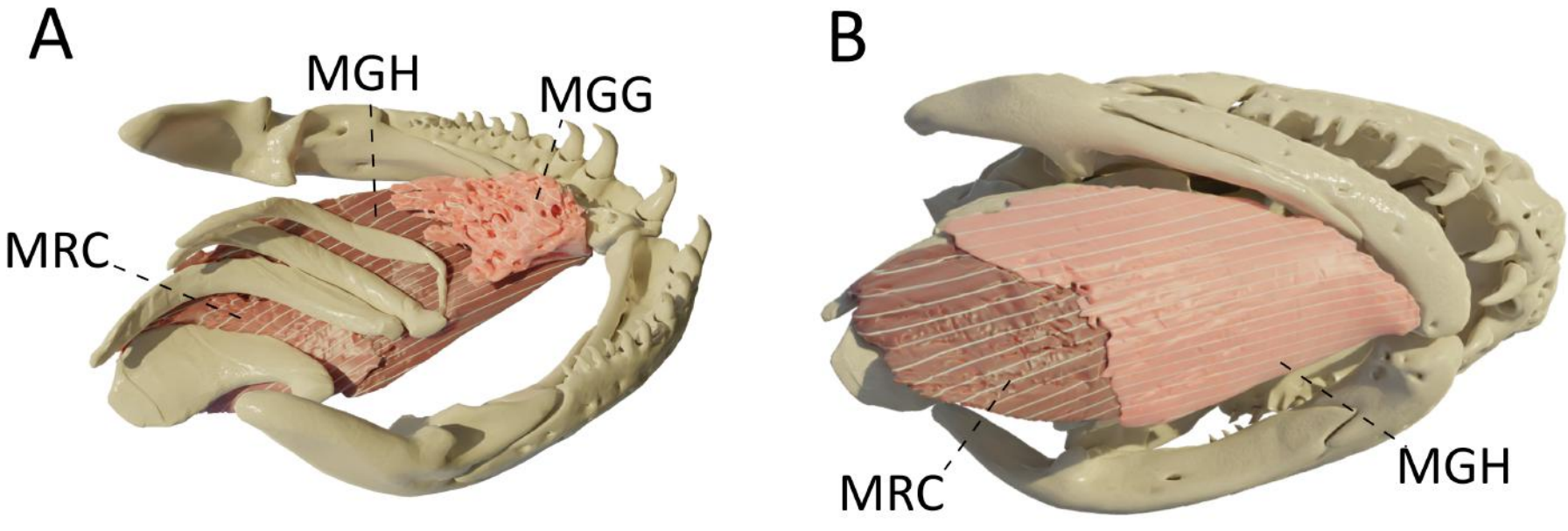
A
MGH
MGG
MRC
B
MRC
MGH

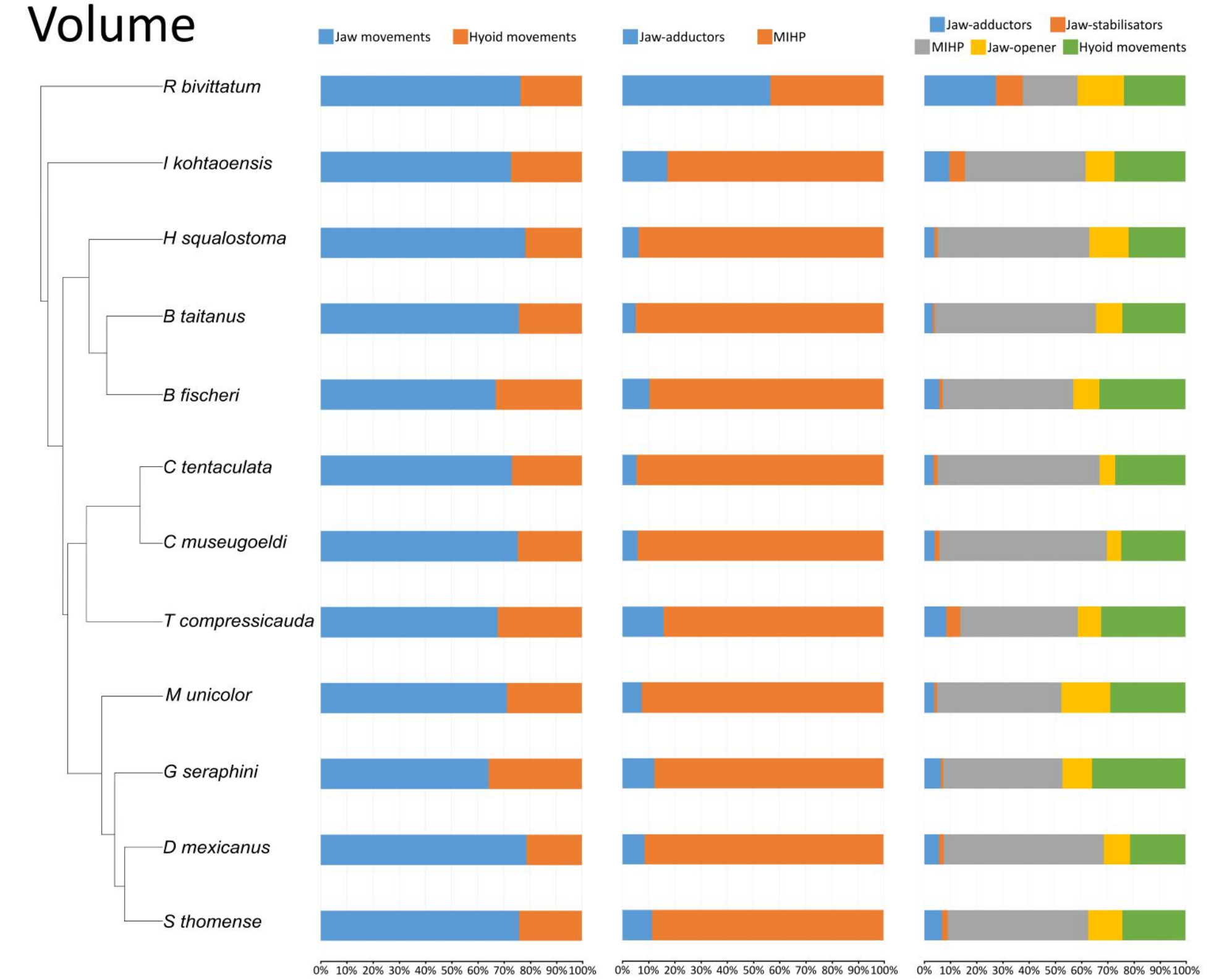
Volume
Jaw movements
Hyoid movements
Jaw-adductors
MIHP
Jaw-adductors
Jaw-stabilisators
MIHP
Jaw-opener
Hyoid movements
R bivittatum
I kohtaoensis
H squalostoma
B taitanus
B fischeri
C tentaculata
C museugoeldi
T compressicauda
M unicolor
G seraphini
D mexicanus
S thomense
0% 10% 20% 30% 40% 50% 60% 70% 80% 90% 100%
0% 10% 20% 30% 40% 50% 60% 70% 80% 90% 100%
0% 10% 20% 30% 40% 50% 60% 70% 80% 90% 100%

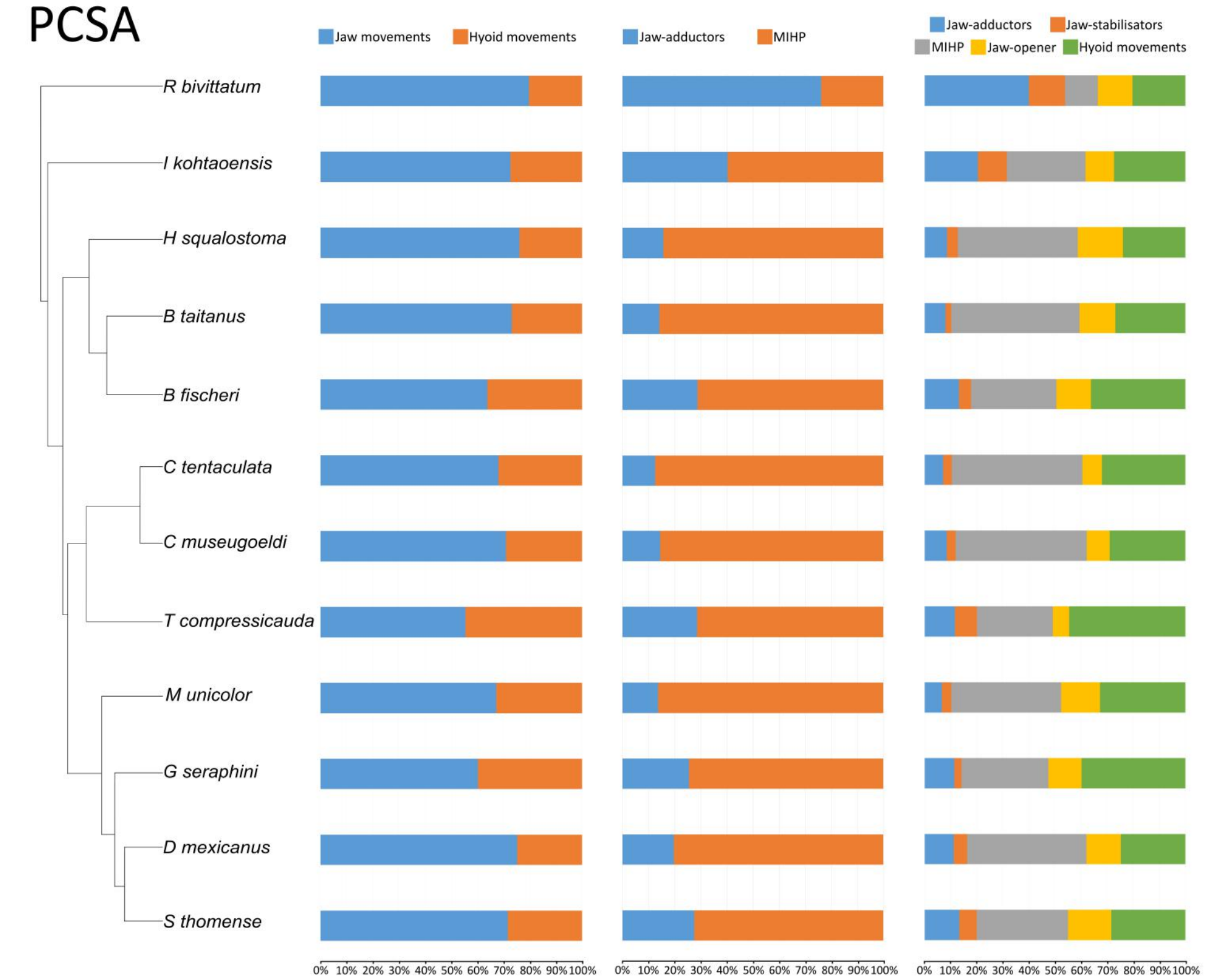
PCSA
Jaw movements
Hyoid movements
Jaw-adductors
MIHP
Jaw-adductors
Jaw-stabilisators
MIHP
Jaw-opener
Hyoid movements
R bivittatum
I kohtaoensis
H squalostoma
B taitanus
B fischeri
C tentaculata
C museugoeldi
T compressicauda
M unicolor
G seraphini
D mexicanus
S thomense
0% 10% 20% 30% 40% 50% 60% 70% 80% 90% 100%
0% 10% 20% 30% 40% 50% 60% 70% 80% 90% 100%
0% 10% 20% 30% 40% 50% 60% 70% 80% 90% 100%

Figure S1. Pruned phylogenetic tree from Jetz and Pyron (2018).

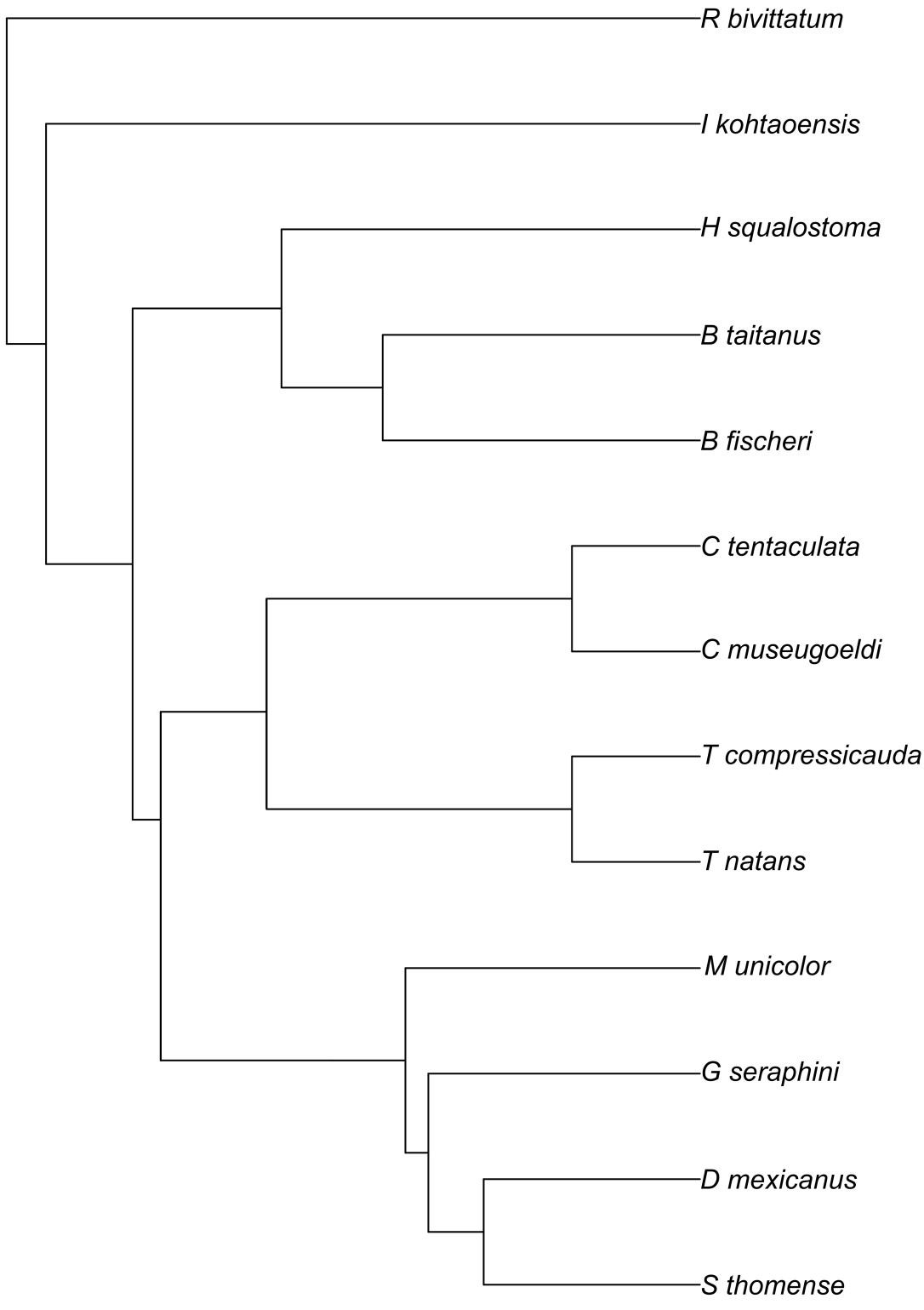

Jetz, W. & Pyron, R.A. (2018). The interplay of past diversification and evolutionary isolation with present imperilment across the amphibian tree of life. *Nat. Ecol. Evol.* **2**, 850–858.

Table S1. Details of the specimens used in the study.

Family	Species	ID
Caeciliidae	*Caecilia museugoeldi*	NHM V2101
	Caecilia tentaculata	NHM 3955
Dermophiidae	*Dermophis mexicanus*	UTACV A-52188
	Dermophis mexicanus	AL AL2101201
	Dermophis mexicanus	AL AL2101202
	Geotrypetes seraphini	AH 2
	Geotrypetes seraphini	AH 6
	Geotrypetes seraphini	AH AL1
	Geotrypetes seraphini	AH AL21
	Geotrypetes seraphini	AH AL5
	Geotrypetes seraphini	AH 5
	Geotrypetes seraphini	AH AL29041901
	Schistometopum thomense	AH 6
	Schistometopum thomense	AH #8
	Schistometopum thomense	AH AL11
Herpelidae	*Boulengerula fischeri*	AH 3
	Boulengerula fischeri	AH 4
	Boulengerula fischeri	AH 5
	Boulengerula fischeri	AH 7
	Boulengerula taitanus	AH JM00519
	Boulengerula taitanus	AH JM00520
	Boulengerula taitanus	AH JM00824
	Boulengerula taitanus	AH JM01029
	Boulengerula taitanus	AH JM01032
	Boulengerula taitanus	AH JM01038
	Boulengerula taitanus	AH JM01040
	Boulengerula taitanus	AH JM01062
	Boulengerula taitanus	AH JM01452
	Boulengerula taitanus	AH JM01584
	Herpele squalostoma	AH AL10
	Herpele squalostoma	AH AL2
	Herpele squalostoma	AH AL30
	Herpele squalostoma	AH AL31
	Herpele squalostoma	AH AL32
Ichthyophiidae	*Ichthyophis kohtaoensis*	UMMZ 218831
	Ichthyophis kohtaoensis	UMMZ 218832
Rhinatrematidae	*Rhinatrema bivittatum*	AH A53
	Rhinatrema bivittatum	AH AL8
	Rhinatrema bivittatum	AH B75
	Rhinatrema bivittatum	AH B80
Siphonopidae	*Microcaecilia unicolor*	AH prey
Typhlonectidae	*Typhlonectes compressicauda*	AH AL6
	Typhlonectes compressicauda	AH AL7
	Typhlonectes natans	SMNS 16297

Abbreviations are as follows: personal collection of Anthony Herrel (AH), personal collection of Aurélien Lowie (AL), Natural History Museum, London (NHM), Staatliches Museum für Naturkunde Stuttgart (SMNS), University of Michigan, Museum of Zoology (UMMZ), University of Texas Arlington, Amphibian & Reptile Diversity Research Center (UTACV)

Table S2. Length (mm), volume (mm³), PCSA (mm²) and pennation angle (deg) of the species included in this study.

Data are means ± standard deviations. n: number of individuals per species; MDM: m. depressor mandibulae, MIHP: m. interhyoideus posterior, MIHA: m. interhyoideus anterior, MAML: m. adductor mandibulae longus, MAMI: m. adductor mandibulae internus, MAMA: m. adductor mandibulae articularis, MIM: m. intermandibularis, MIMP: m. intermandibularis posterior, MGH: m. geniohyoideus, MRC: m. rectus cervicis, MGG: m. genioglossus, MPT: m. pterygoideus, MPTI: m. pterygoideus internus, MLQ: m. levator quadrati.

Species	n	L_MDM	L_MIHP	L_MIHA	L_MAML	L_MAMI	L_MAMA	L_MIM	L_MIMP
Boulengerula fischeri	4	1.179 ± 0.119	2.428 ± 0.277	1.885 ± 0.38	0.736 ± 0.168	0.747	0.48	1.154 ± 0.131	NA
Boulengerula taitanus	10	1.405 ± 0.318	2.306 ± 0.384	2.469 ± 0.559	0.962 ± 0.082	NA	0.653 ± 0.136	1.49 ± 0.303	NA
Caecilia museugoeldi	1	2.243	4.158	3.254	2.03	0.895	1.178	1.917	NA
Caecilia tentaculata	1	4.816	6.656	8.253	3.507	2.464	1.714	5.394	NA
Dermophis mexicanus	3	4.027 ± 0.49	6.59 ± 0.732	5.477 ± 0.424	3.178 ± 0.31	2.09 ± 0.264	1.585 ± 0.496	4.291 ± 0.565	NA
Geotrypetes seraphini	7	1.661 ± 0.47	2.836 ± 1.248	2.314 ± 0.759	1.188 ± 0.419	1.179 ± 0.49	0.823	1.346 ± 0.425	1.745 ± 0.644
Herpele squalostoma	5	1.96 ± 0.291	2.595 ± 0.527	2.861 ± 0.536	1.128 ± 0.134	0.903 ± 0.274	0.759	2.097 ± 0.463	NA
Ichthyophis kohtaoensis	2	3.158 ± 0.18	4.737 ± 0.57	3.454 ± 1.873	1.812 ± 0.1	1.477 ± 0.085	0.931 ± 0.113	2.658 ± 0.271	NA
Microcaecilia unicolor	1	1.569	1.192	1.273	0.834	0.434	0.361	0.814	NA
Rhinatrema bivittatum	4	1.793 ± 0.524	2.342 ± 0.662	2.301 ± 0.255	0.83 ± 0.222	1.075 ± 0.08	1.259 ± 0.164	1.806 ± 0.512	NA
Schistometopum thomense	3	1.975 ± 0.271	3.629 ± 0.42	2.027 ± 0.855	1.457 ± 0.354	0.839 ± 0.327	1.302 ± 0.661	1.531 ± 0.28	NA
*Typhlonectes compressicauda**	3	4.121 ± 1.05	4.079 ± 1.517	4.024 ± 0	2.158 ± 0.426	1.862 ± 0.665	1.724	2.843 ± 0.353	NA

Species	L_MGH	L_MRC	L_MGG	L_MPT	L_MPTI	L_MLQ
Boulengerula fischeri	1.897 ± 0.183	1.892 ± 0.178	0.668 ± 0.195	0.627 ± 0.18	NA	0.352
Boulengerula taitanus	2.018 ± 0.207	1.805 ± 0.355	0.649 ± 0.154	0.886 ± 0.262	NA	0.268
Caecilia museugoeldi	5.515	3.359	1.128	2.233	NA	0.706
Caecilia tentaculata	7.591	5.322	1.343	3.12	NA	1.344
Dermophis mexicanus	6.728 ± 1.124	5.218 ± 0.855	2.315 ± 1.127	2.295 ± 0.976	NA	1.34 ± 0.171
Geotrypetes seraphini	2.337 ± 0.998	1.879 ± 0.541	1.106 ± 0.509	0.528 ± 0.154	NA	0.716
Herpele squalostoma	3.209 ± 0.518	1.706 ± 0.422	0.913 ± 0.522	0.914 ± 0.203	NA	0.491
Ichthyophis kohtaoensis	6.023 ± 1.196	5.239 ± 0.464	1.347 ± 0.192	1.8 ± 0.253	0.759	1.097 ± 0.367
Microcaecilia unicolor	1.479	1.923	0.691	0.375	NA	0.398
Rhinatrema bivittatum	1.974 ± 0.577	2.054 ± 0.848	0.671 ± 0.104	1.033 ± 0.43	0.744	NA
Schistometopum thomense	3.311 ± 0.64	2.683 ± 0.363	1.109 ± 0.373	1.069 ± 0.494	NA	0.666
*Typhlonectes compressicauda**	3.855 ± 1.714	2.761 ± 0.826	0.671 ± 0.533	1.656 ± 0.73	NA	NA

Species	V_MDM	V_MIHP	V_MIHA	V_MAML	V_MAMI	V_MAMA	V_MIM	V_MIMP	V_MGH
Boulengerula fischeri	0.188 ± 0.118	0.944 ± 0.356	0.257 ± 0.049	0.101 ± 0.033	0.004 ± 0.001	0.003 ± 0.001	0.103 ± 0.029	NA	0.1 ± 0.035
Boulengerula taitanus	0.979 ± 0.252	5.964 ± 2.635	0.805 ± 0.236	0.226 ± 0.11	NA	0.092 ± 0.043	0.733 ± 0.35	NA	0.359 ± 0.124
Caecilia museugoeldi	3.859	45.129	4.67	2.236	0.366	0.167	2.43	NA	5.584
Caecilia tentaculata	19.624	200.886	33.77	8.041	2.237	1.121	14.702	NA	20.5
Dermophis mexicanus	18.593 ± 8.514	113.996 ± 65.291	6.401 ± 4.863	7.749 ± 3.126	2.171 ± 0.986	0.654 ± 0.463	7.921 ± 4.684	NA	9.247 ± 2.224
Geotrypetes seraphini	1.393 ± 0.535	5.615 ± 2.108	1.108 ± 0.537	0.576 ± 0.162	0.141 ± 0.067	0.064	1.001 ± 0.624	0.399 ± 0.119	0.819 ± 0.345
Herpele squalostoma	2.239 ± 0.925	8.645 ± 2.805	0.685 ± 0.521	0.399 ± 0.133	0.145 ± 0.034	0.029	0.876 ± 0.541	NA	0.881 ± 0.312
Ichthyophis kohtaoensis	1.881 ± 0.189	7.791 ± 2.027	0.295 ± 0.004	0.893 ± 0.412	0.42 ± 0.218	0.311 ± 0.108	1.716 ± 0.349	NA	1.181 ± 0.38
Microcaecilia unicolor	1.081	2.753	0.447	0.185	0.022	0.012	0.169 ± 0.055	NA	0.489 ± 0.109
Rhinatrema bivittatum	1.677 ± 0.707	1.985 ± 0.822	0.137 ± 0.189	1.918 ± 0.955	0.223 ± 0.07	0.441 ± 0.16	0.713 ± 0.261	NA	0.585 ± 0.333
Schistometopum thomense	1.628 ± 0.981	6.67 ± 4.377	0.719 ± 0.774	0.514 ± 0.4	0.225 ± 0.216	0.107	0.41 ± 0.347	NA	0.815 ± 0.822
*Typhlonectes compressicauda**	2.91 ± 1.117	14.601 ± 8.491	2.397	1.804 ± 1.126	0.568725101	0.368	2.271 ± 0.558	NA	1.65 ± 1.248

Species	V_MRC	V_MGG	V_MPT	V_MPTI	V_MLQ
Boulengerula fischeri	0.113 ± 0.023	0.05 ± 0.009	0.017 ± 0.012	NA	0.008
Boulengerula taitanus	0.312 ± 0.1	0.123 ± 0.047	0.056 ± 0.058	NA	0.015
Caecilia museugoeldi	3.659	0.964	1.311	NA	0.058
Caecilia tentaculata	10.424	7.755	5.055	NA	0.223
Dermophis mexicanus	8.873 ± 2.988	7.034 ± 8.318	2.63 ± 1.32	NA	0.73 ± 0.241
Geotrypetes seraphini	0.82 ± 0.399	0.251 ± 0.361	0.047 ± 0.033	NA	0.064
Herpele squalostoma	0.522 ± 0.168	0.171 ± 0.089	0.142 ± 0.055	NA	0.054
Ichthyophis kohtaoensis	0.858 ± 0.171	0.533 ± 0.277	0.935 ± 0.247	0.015	0.064 ± 0.024
Microcaecilia unicolor	0.305 ± 0.062	0.254	0.036	NA	0.029 ± 0.012
Rhinatrema bivittatum	0.601 ± 0.376	0.187 ± 0.186	0.858 ± 0.406	0.111	NA
Schistometopum thomense	0.61 ± 0.588	0.44 ± 0.68	0.163 ± 0.091	NA	0.111
*Typhlonectes compressicauda**	1.491 ± 0.48	2.65	1.744 ± 1.586	NA	NA

Species	PCSA_MDM	PCSA_MIHP	PCSA_MIHA	PCSA_MAML	PCSA_MAMI	PCSA_MAMA	PCSA_MIM	PCSA_MIMP	PCSA_MGH
Boulengerula fischeri	0.154 ± 0.082	0.38 ± 0.177	0.139 ± 0.029	0.141 ± 0.044	0.006	0.007	0.089 ± 0.025	NA	0.053 ± 0.016
Boulengerula taitanus	0.695 ± 0.061	2.481 ± 1.4	0.327 ± 0.081	0.267 ± 0.114	NA	0.139 ± 0.062	0.484 ± 0.208	NA	0.175 ± 0.051
Caecilia museugoeldi	1.721	9.796	1.435	1.101	0.41	0.142	1.268	NA	1.012
Caecilia tentaculata	4.074	27.026	4.092	2.293	0.908	0.654	2.725	NA	2.701
Dermophis mexicanus	4.542 ± 1.695	15.791 ± 8.933	1.207 ± 0.981	2.393 ± 0.715	1.017 ± 0.355	0.454 ± 0.412	1.776 ± 0.805	NA	1.365 ± 0.115
Geotrypetes seraphini	0.842 ± 0.208	2.214 ± 1.251	0.526 ± 0.283	0.539 ± 0.235	0.139 ± 0.06	0.078 ± 0	0.797 ± 0.435	0.231 ± 0.157	0.384 ± 0.169
Herpele squalostoma	1.131 ± 0.378	2.994 ± 0.863	0.3 ± 0.196	0.351 ± 0.105	0.171 ± 0.062	0.038 ± 0	0.441 ± 0.315	NA	0.27 ± 0.067
Ichthyophis kohtaoensis	0.596 ± 0.056	1.645 ± 0.441	0.1 ± 0.053	0.49 ± 0.213	0.279 ± 0.134	0.344 ± 0.151	0.642 ± 0.07	NA	0.201 ± 0.078
Microcaecilia unicolor	0.69	1.955	0.351	0.224	0.052	0.033	0.273	NA	0.37
Rhinatrema bivittatum	0.975 ± 0.381	0.92 ± 0	0.151 ± 0.032	2.358 ± 0.99	0.22 ± 0.077	0.354 ± 0.145	0.407 ± 0.125	NA	0.304 ± 0.159
Schistometopum thomense	0.795 ± 0.384	1.678 ± 1.068	0.299 ± 0.227	0.331 ± 0.183	0.242 ± 0.185	0.064 ± 0.09	0.256 ± 0.216	NA	0.22 ± 0.182
*Typhlonectes compressicauda**	0.693 ± 0.148	3.211 ± 0.697	0.596 ± 0	0.814 ± 0.397	0.258 ± 0.205	0.213 ± 0	0.79 ± 0.103	NA	0.445 ± 0.235

Species	PCSA_MRC	PCSA_MGG	PCSA_MPT	PCSA_MPTI	PCSA_MLQ
Boulengerula fischeri	0.061 ± 0.016	0.079 ± 0.026	0.032 ± 0.026	NA	0.022
Boulengerula taitanus	0.173 ± 0.041	0.194 ± 0.078	0.055 ± 0.044	NA	0.055
Caecilia museugoeldi	1.089	0.855	0.587	NA	0.082
Caecilia tentaculata	1.959	5.773	1.62	NA	0.166
Dermophis mexicanus	1.678 ± 0.369	2.532 ± 1.97	1.216 ± 0.55	NA	0.547 ± 0.183
Geotrypetes seraphini	0.464 ± 0.246	0.243 ± 0.324	0.093 ± 0.062	NA	0.09
Herpele squalostoma	0.319 ± 0.11	0.192 ± 0.065	0.16 ± 0.074	NA	0.11
Ichthyophis kohtaoensis	0.165 ± 0.039	0.385 ± 0.17	0.522 ± 0.125	0.02	0.066 ± 0.037
Microcaecilia unicolor	0.158	0.368	0.097	NA	0.071
Rhinatrema bivittatum	0.321 ± 0.265	0.306 ± 0.333	0.873 ± 0.402	0.149	NA
Schistometopum thomense	0.224 ± 0.215	0.359 ± 0.523	0.151 ± 0.069	NA	0.166
*Typhlonectes compressicauda**	0.552 ± 0.156	2.528 ± 0	0.922 ± 0.471	NA	NA

*** Due to the scarcity of Typhlonectes compressicauda in the collections but the availability of Typhlonectes natans, the mean for T. compressicauda includes one specimen of T. natans. As the species are morphologically and phylogenetically close, we assumed that the data would not be biased by this addition.**

species	MIHP angle				MAMI angle			
	Mean	Min	Max	SD	Mean	Min	Max	SD
Boulengerula fischeri	20.13	5.55	32	8.87	NA	NA	NA	NA
Boulengerula taitanus	23.19	12.46	37.11	8.8	NA	NA	NA	NA
Caecilia museugoeldi	25.49	5.55	60.57	15.23	NA	NA	NA	NA
Caecilia tentaculata	26.43	8.75	60.11	14.36	NA	NA	NA	NA
Dermophis mexicanus	25.1	10.16	66.33	18.26	NA	NA	NA	NA
Geotrypetes seraphini	19.48	4.87	39.64	11.76	NA	NA	NA	NA
Herpele squalostoma	25.54	4.4	61.52	16.12	NA	NA	NA	NA
Ichthyophis kohtaoensis	5.67	0.33	16.69	6.95	NA	NA	NA	NA
Microcaecilia unicolor	38.8	11.17	63.67	13.99	NA	NA	NA	NA
Rhinatrema bivittatum	NA	NA	NA	NA	117.61	108.44	129.54	6.48
Schistometopum thomense	21.17	13.74	25.96	3.66	NA	NA	NA	NA
Typhlonectes natans	20.18	12.35	27.97	5.07	NA	NA	NA	NA

Table S3. Details of the scanned specimens used in this study.

Family	Species	ID	Staining	Untreated voxel size (µm)	Stained voxel size (µm)
Caeciliidae	*Caecilia museugoeldi*	NHM V2101	I_2KI	17.65	16.61
	Caecilia tentaculata	NHM 3955	I_2KI	22.93	14.01
Dermophiidae	*Dermophis mexicanus*	UTACV A-52188	PMA	23.05	9.58
	Geotrypetes seraphini	AH 6	PMA	15.17	4
	Schistometopum thomense	AH #8	PMA	16	7.04
Herpelidae	*Boulengerula fischeri*	AH 5	PMA	9.8	5.49
	Boulengerula taitanus	AH JM01452	PMA	12.23	7.04
	Herpele squalostoma	AH AL31	PMA	13.53	10.49
Ichthyophiidae	*Ichthyophis kohtaoensis*	UMMZ 218831	I_2KI	14.29	6.41
Rhinatrematidae	*Rhinatrema bivittatum*	AH AL8	PMA	16.69	9.59
Siphonopidae	*Microcaecilia unicolor*	AH prey	I_2KI	9.24	5
Typhlonectidae	*Typhlonectes natans*	SMNS 16297	I_2KI	11.06	10

Abbreviations are as follows:

Personal collection of Anthony Herrel (AH)
Natural History Museum, London (NHM)
Staatliches Museum für Naturkunde Stuttgart (SMNS)
University of Michigan, Museum of Zoology (UMMZ)
University of Texas Arlington, Amphibian & Reptile Diversity Research Center (UTACV)

Lugol's iodine (I_2KI)
Phosphomolybdic acid (PMA)